SoftCOM '18
tutorials

Mathematical Modelling with Applications in Antenna Theory, EMC and Actuarial Mathematics

by

Milica Rančić

Mälardalen University, UKK, Division of Applied Mathematics, Västerås, Sweden

September 13 - 15, 2018.

Mathematical Modelling with Applications in Antenna Theory, EMC and Actuarial Mathematics

presenter: Milica Rančić

Mälardalen University, Division of Applied Mathematics, Västerås, Sweden

September 2018

Outline

Tutorial is organised in three parts:

- PART I - Modelling Related to Antenna Theory, Grounding Systems, and related
- PART II - Modelling of Lightning and Electrostatic Discharge Currents
- PART III - Modelling of Mortality Rates of Living Organisms or Equipment

- Using the `full-wave approach` for analysis of wire conductors above or buried in semi-conducting ground:
  - any kind of arbitrarily positioned wire system can be analyzed,
  - at any frequency of interest,
  - with no restrictions to the electrical parameters of the ground.
- This approach is based on formulation of the `electric field integral equation (EFIE)` and its solution using an appropriate numerical method.
- The influence of ground parameters is taken into account through `Sommerfeld integrals`, which are a part of the kernel of the formulated integral equation (e.g. Hallén IE Pocklington IE, etc.).
- High calculation accuracy, but greater computational cost to be paid

Wire Antenna Structures Above Lossy Ground

- Vertical/Horizontal Dipole Antennas,
- Vertical Monopole Antennas,
- Coupled Wire Antennas (Horizontal, Verical, Monopoles),
- Yagi structures,
- etc.

Horizontal dipole antenna (HDA) above lossy half-space (LHS)

Results have been obtained applying the point-matching method (PMM) to solve the system of Hallen's integral equations. Polynomial current approximation is adopted.

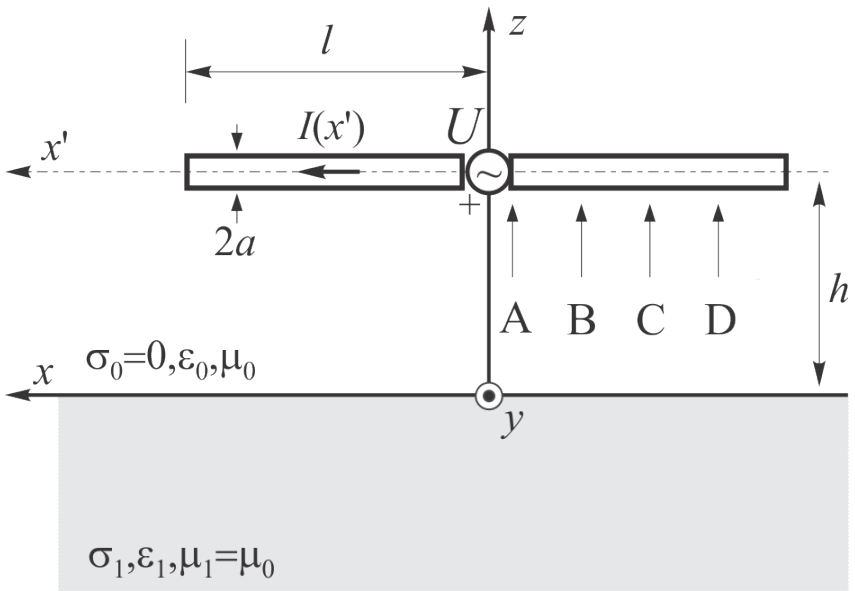

Figure: HDA above LHS

Horizontal dipole antenna above LHS

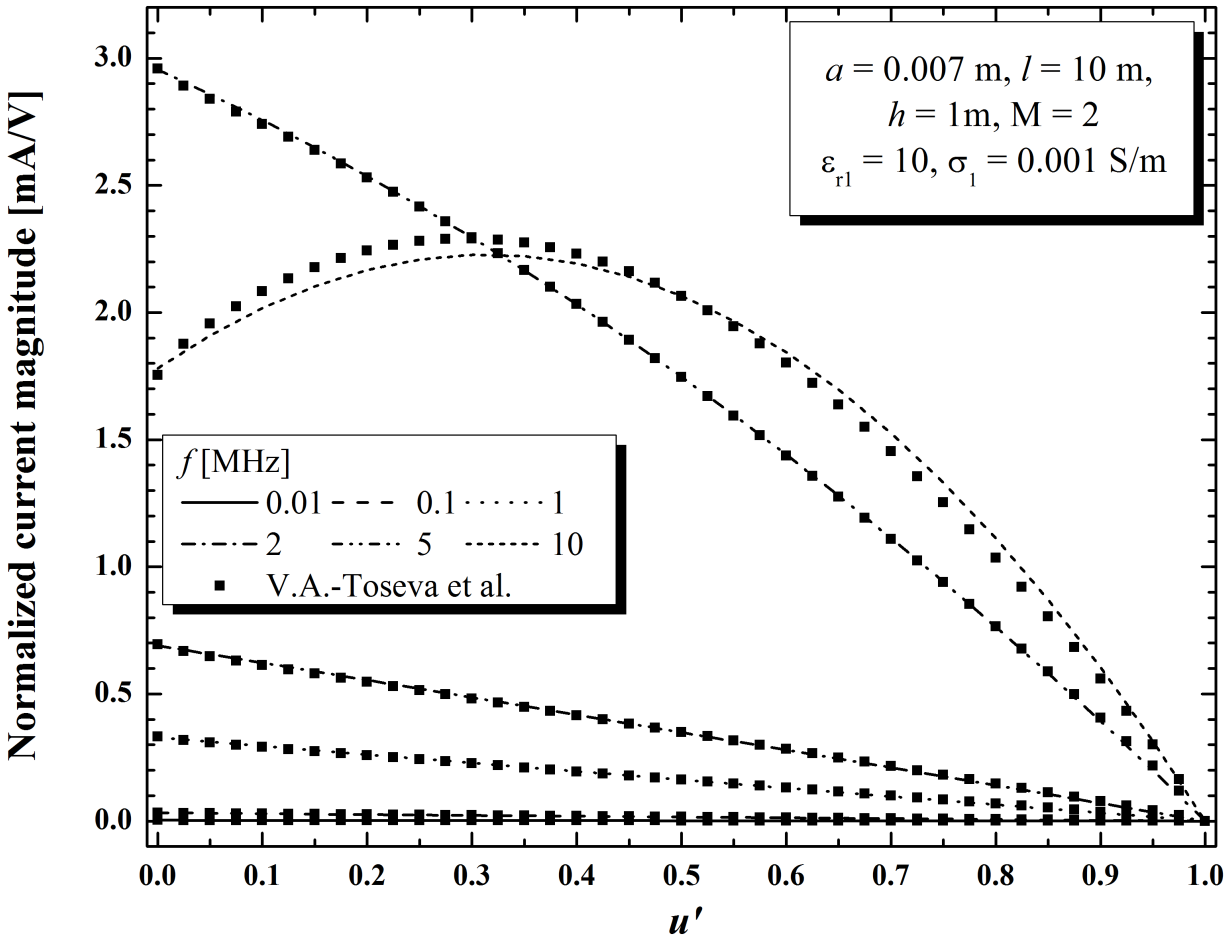

Figure: Comparison with full-wave approach

Horizontal dipole antenna above LHS

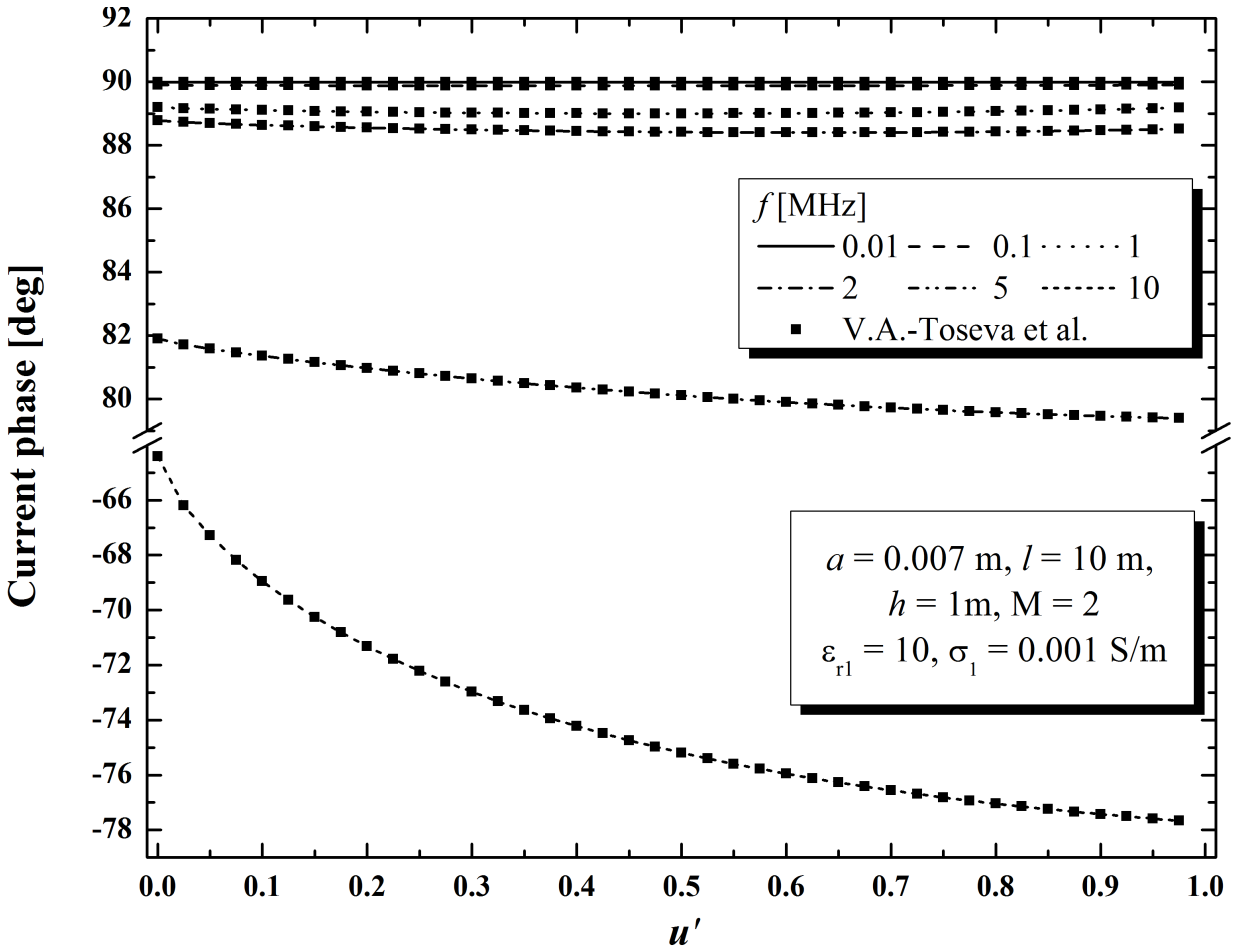

Figure: Comparison with full-wave approach

Horizontal dipole antenna above LHS

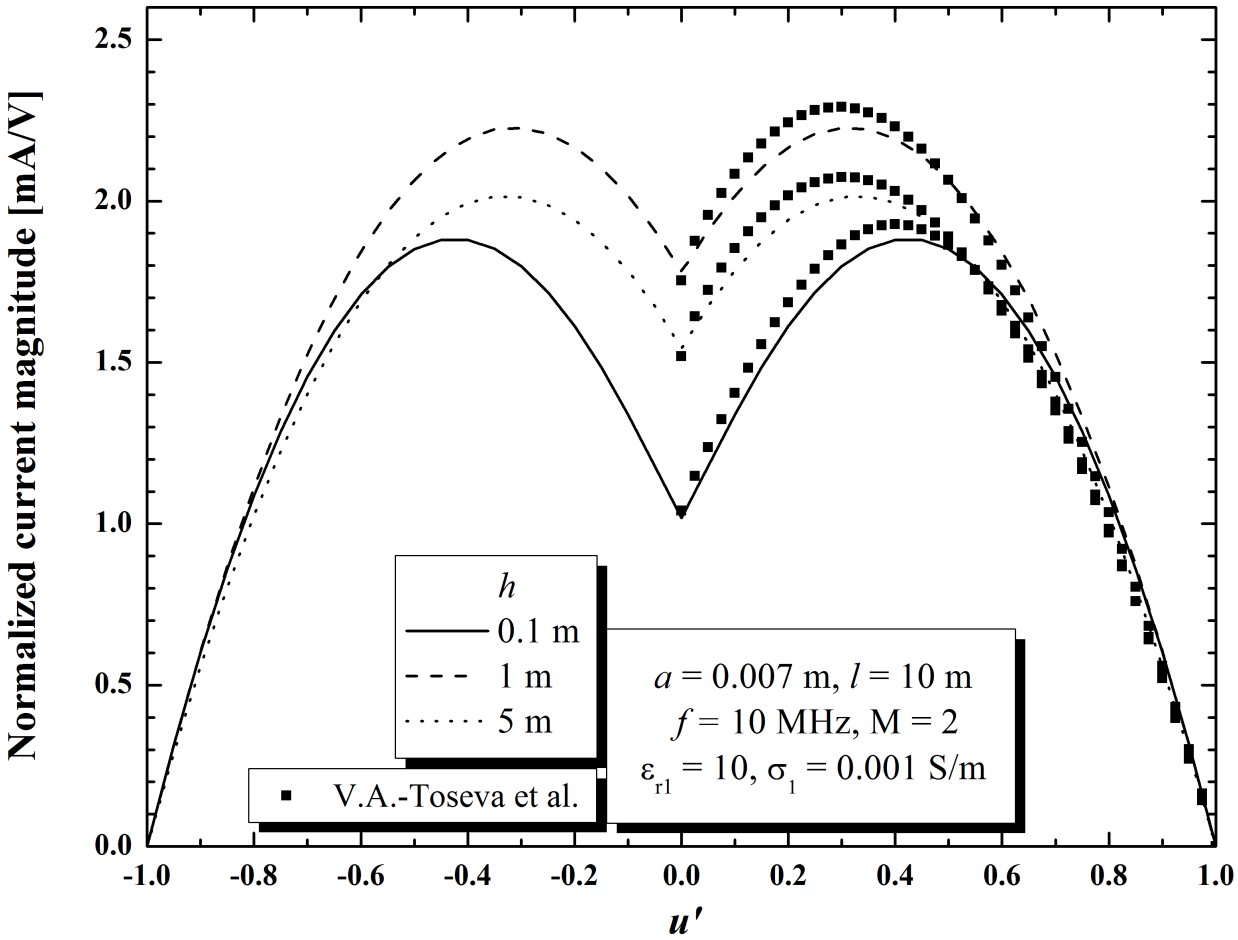

Figure: Comparison with full-wave approach

Horizontal dipole antenna above LHS

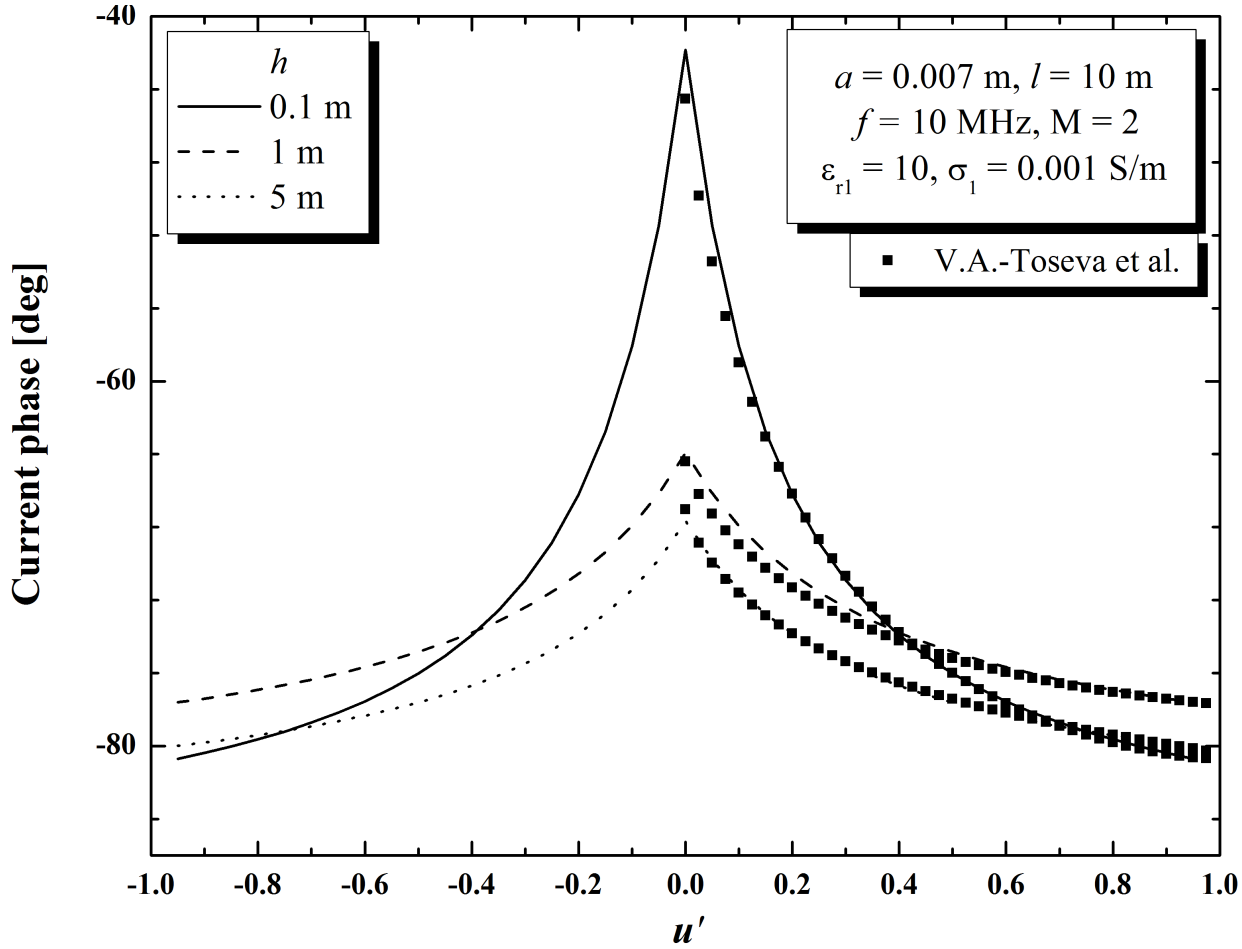

Figure: Comparison with full-wave approach

Horizontal dipole antenna above LHS

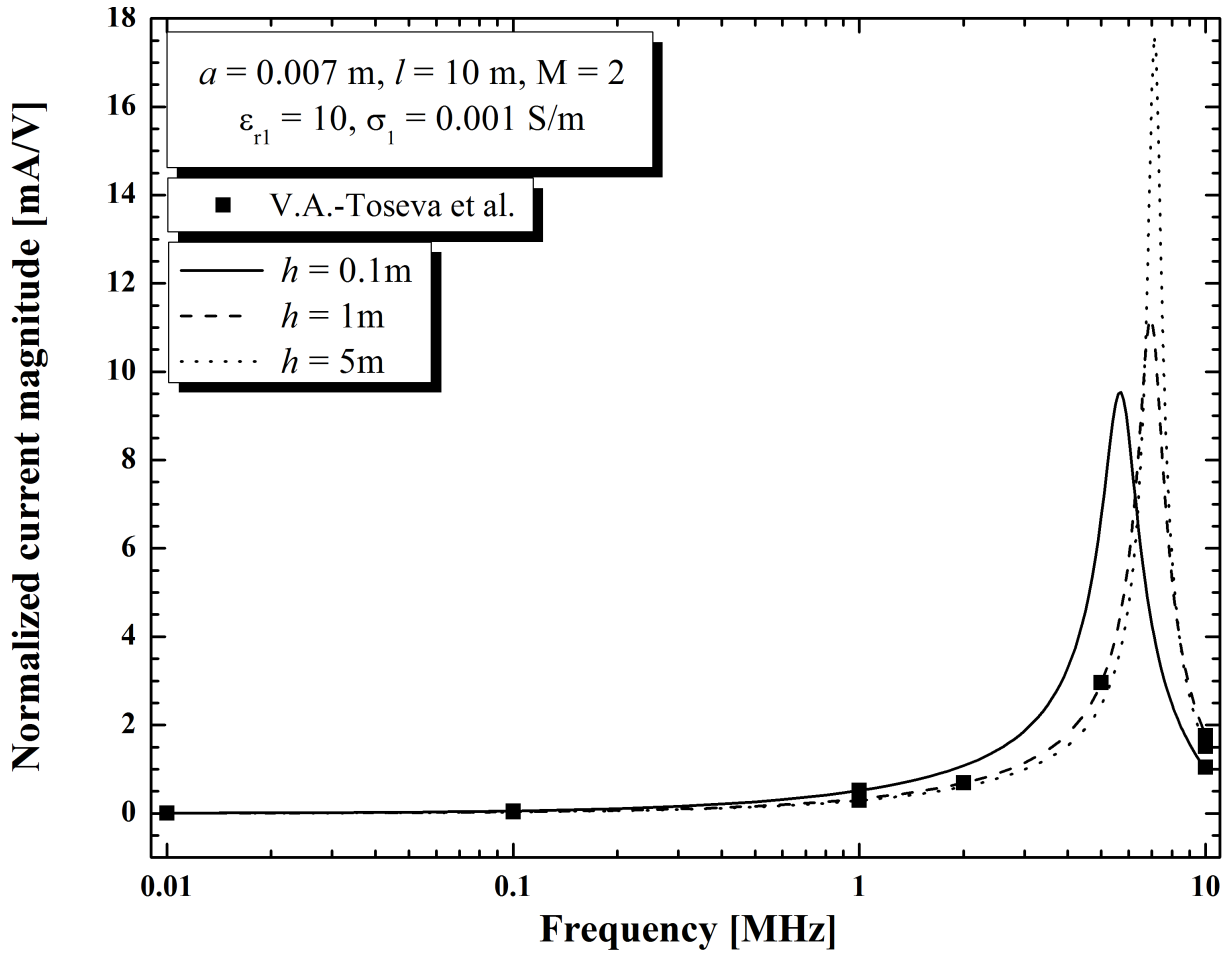

Figure: Comparison with full-wave approach

Horizontal dipole antenna above LHS

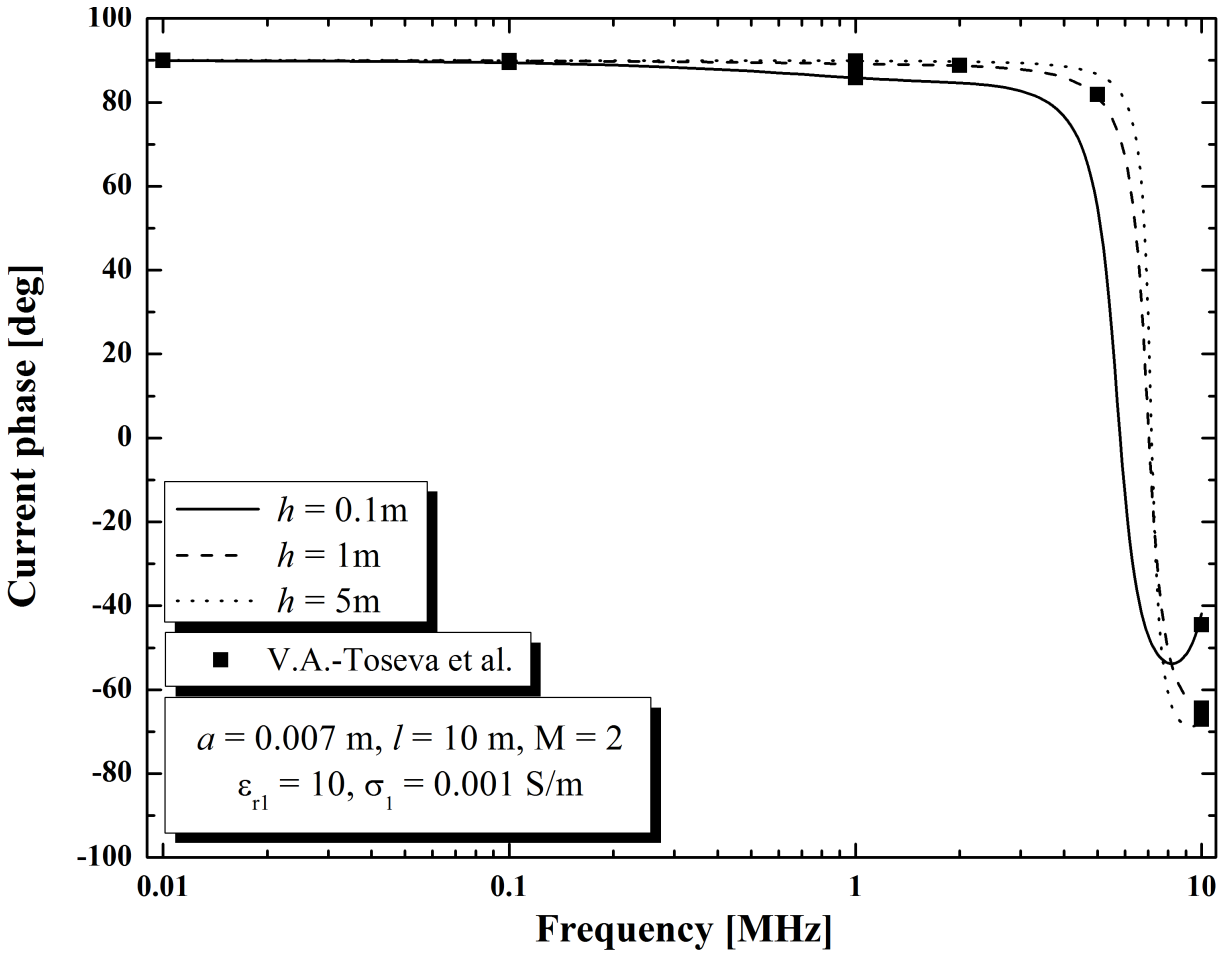

Figure: Comparison with full-wave approach

Horizontal dipole antenna above LHS

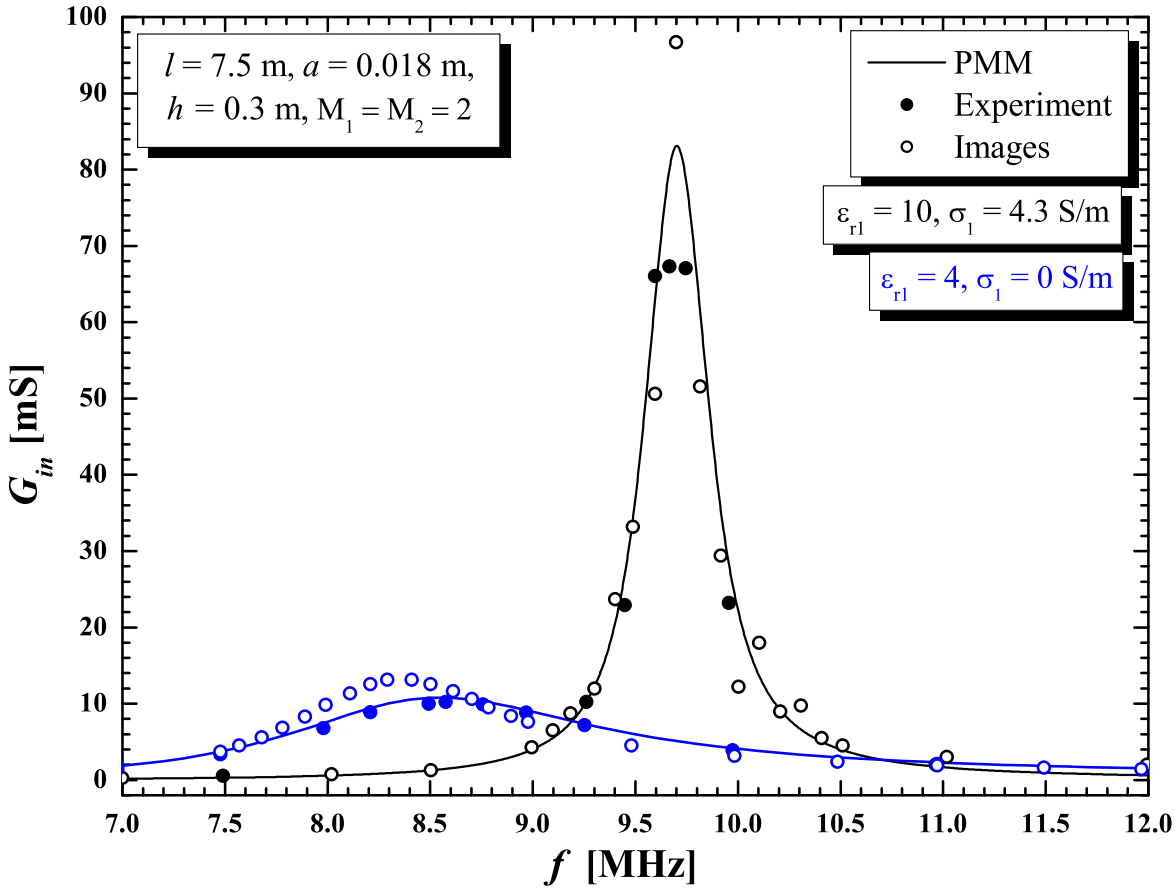

Figure: Comparison with measured data and method of images

Horizontal dipole antenna above LHS

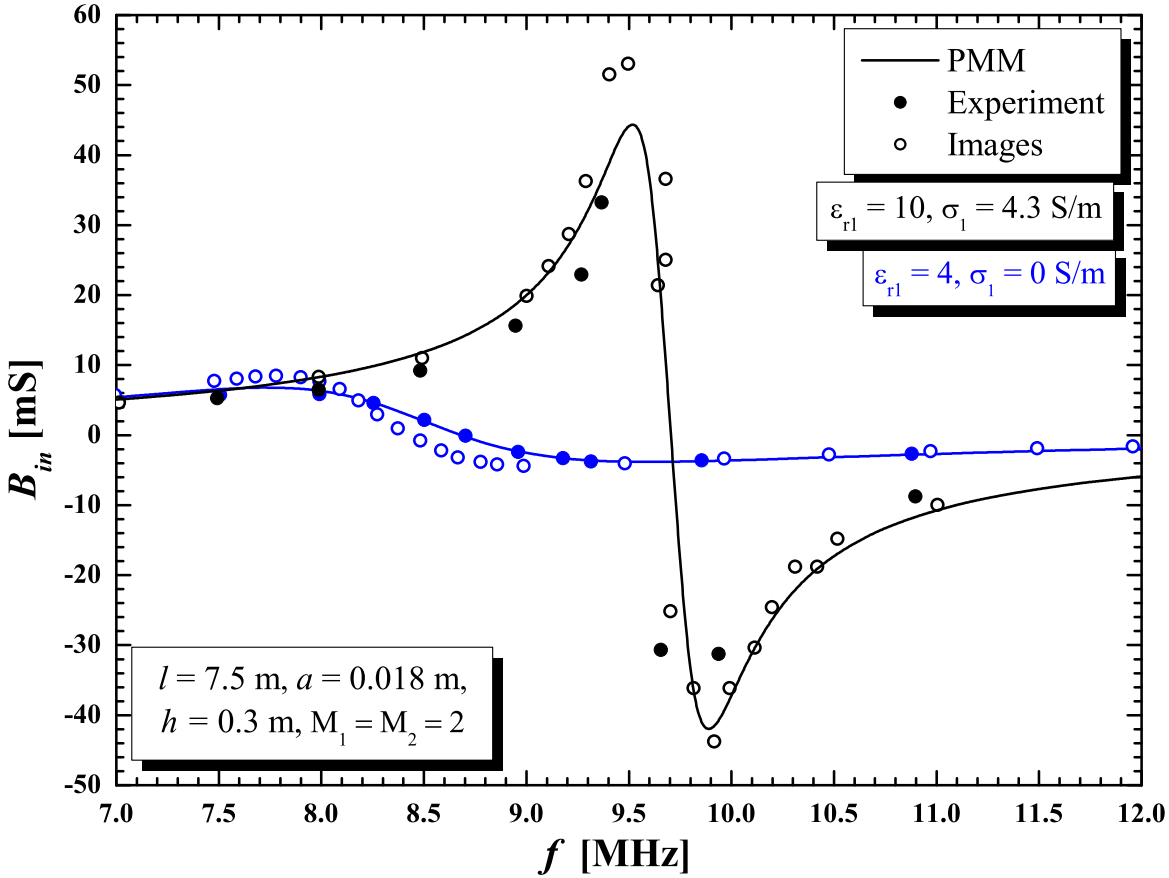

Figure: Comparison with measured data and method of images

Sources Buried in the Lossy Half-space

- Grounding systems,
- Buried antennas,
- Buried telecommunication cables exposed to EM interferences,
- Bare or isolated antennas embedded in dissipative media,
- etc.

In all these cases few forms of Sommerfeld integrals occur.

Horizontal conductor buried in LHS

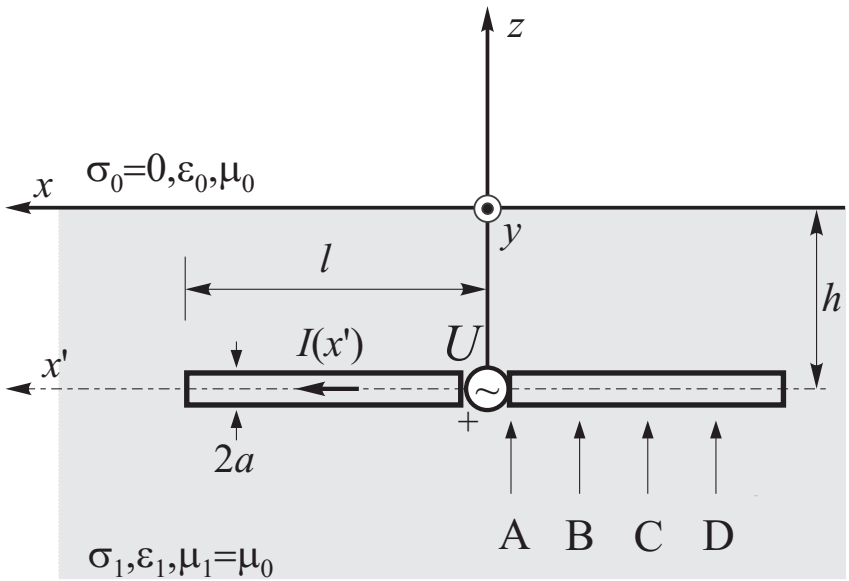

The Hertz's vector potential: $\mathbf{\Pi}_1 = \Pi_{x1}\hat{x} + \Pi_{z1}\hat{z}$

Horizontal conductor buried in LHS

Tangential component of the scattered electric field:

$$E_{x1}^{sct}(x,x') = \left[\frac{\partial^2}{\partial x^2} - \underline{\gamma}_1^2\right]\Pi_{x1} + \frac{\partial^2 \Pi_{z1}}{\partial x \partial z}, \tag{1}$$

where

$$\Pi_{x1} = \frac{1}{4\pi\underline{\sigma}_1}\int_{-l}^{l} I(x')\left[K_o(x,x') - K_i(x,x') + U_{11}\right]\mathrm{d}x', \tag{2}$$

$$\Pi_{z1} = \frac{1}{4\pi\underline{\sigma}_1}\int_{-l}^{l} I(x')\frac{\partial W_{11}}{\partial x}\mathrm{d}x', \tag{3}$$

with $I(x')$ - the current distribution along the conductor

Horizontal conductor buried in LHS

Adopting (2) and (3), expression (1) can be written as

$$E_{x1}^{sct}(x,x') = \frac{1}{4\pi\underline{\sigma}_1}\int_{-l}^{l} I(x')G(x,x')\mathrm{d}x', \tag{4}$$

$$G(x,x') = \left[\frac{\partial^2}{\partial x^2} - \underline{\gamma}_1^2\right]\left[K_o(x,x') - K_i(x,x') + U_{11}\right] + \frac{\partial^2}{\partial x \partial z}\left[\frac{\partial W_{11}}{\partial x}\right]. \tag{5}$$

Now, integral denoted by W_{11} can be rewritten as
$\frac{\partial W_{11}}{\partial z} = -\underline{\gamma}_1^2 V_{11} - U_{11}$

Horizontal conductor buried in LHS

$$E_{x1}^{sct}(x,x') = \frac{1}{4\pi\underline{\sigma}_1}\left[\begin{array}{l} \frac{\partial^2}{\partial x^2}\int_{-l}^{l} I(x')\left[K_o(x,x') - K_i(x,x') - \underline{\gamma}_1^2 V_{11}\right]\mathrm{d}x' - \\ \\ -\underline{\gamma}_1^2\int_{-l}^{l} I(x')\left[K_o(x,x') - K_i(x,x') + U_{11}\right]\mathrm{d}x' \end{array}\right] \tag{6}$$

$$K_o(x,x') = e^{-\underline{\gamma}_1 r_o}/r_0,\ r_o = \sqrt{\rho^2 + a^2},\ \rho = |x - x'|,$$
$$K_i(x,x') = e^{-\underline{\gamma}_1 r_i}/r_1,\ r_i = \sqrt{\rho^2 + (2h)^2},\ \rho = |x - x'|,$$

$$\underline{\gamma}_i = \alpha_i + j\beta_i = (j\omega\mu_i\underline{\sigma}_i)^{1/2},$$
$$\underline{\sigma}_i = \sigma_i + j\omega\epsilon_1,\ \omega = 2\pi f,\ \epsilon_1 = \epsilon_{r1}\epsilon_0,\ \mu_1 = \mu_0,$$
$$\underline{n} = \gamma_1/\gamma_0 = \epsilon_{r1}^{1/2} = (\epsilon_{r1} - j60\sigma_1\lambda_0)^{1/2}.$$

Horizontal conductor buried in LHS

Boundary condition for the total tangential component of the electric field vector

$$E_{x1}^{sct}(x, x') + E_{x1}^{tr}(x, x') = 0, \tag{7}$$

where $E_{x1}^{tr}(x, x')$ is the transmitted electric field.
For the case of a thin-wire conductor centrally-fed by a Dirac's δ-generator,

$$E_{x1}^{tr}(x, x') = U\delta(x), \quad U = 1 \text{ V}$$

which gives an integral equation that needs to be solved numerically. This will involve approximation of Sommerfeld's Integrals U_{11} and V_{11}.

Horizontal conductor buried in LHS

Different approaches applied; most of them start with a simplified version of the Green's function

$$G(x,x') = \left[\frac{\partial^2}{\partial x^2} - \underline{\gamma}_1^2\right]\left[K_o(x,x') - K_i(x,x') + U_{11}\right] + \frac{\partial^2}{\partial x \partial z}\left[\frac{\partial W_{11}}{\partial x}\right]$$

Simplified:

$$G(x,x') = \left[\frac{\partial^2}{\partial x^2} - \underline{\gamma}_1^2\right]\left[K_o(x,x') - K_i(x,x') + U_{11}\right] \qquad (8)$$

only one Sommerfeld integral (U_{11}) needs to be solved

Sommerfeld integral

$$U_{11} = \int_{\alpha=0}^{\infty} \tilde{T}_{\eta 1}(\alpha) e^{-u_1(z+h)} \frac{\alpha}{u_1} J_0(\alpha\rho) \mathrm{d}\alpha \tag{9}$$

where $J_0(\alpha\rho)$ - zero-order Bessel function of the first kind, and

$$\tilde{T}_{\eta 1}(\alpha) = \frac{2u_1}{u_0 + u_1}, \;\; u_i = \sqrt{\alpha^2 + \underline{\gamma}_i^2}, \;\; i = 0, 1 \tag{10}$$

Prudnikov et al. [4]

$$\int_{\alpha=0}^{\infty} \frac{e^{-|c|\sqrt{\alpha^2+\underline{\gamma}_1^2}}}{\sqrt{\alpha^2 + \underline{\gamma}_1^2}} \alpha \; J_0(\alpha\rho) \mathrm{d}\alpha = K_c(x, x') = \frac{e^{-\underline{\gamma}_1\sqrt{\rho^2+|c|^2}}}{\sqrt{\rho^2 + |c|^2}},$$

Proposed model - Case 1

Let us assume (9) in the following form

$$\tilde{T}^{a}_{\eta 1} = \underline{B} + \underline{A} e^{-(u_1 - \underline{\gamma}_1)\underline{d}}. \tag{11}$$

$$U^{a}_{11} = \underline{B} K_{zh}(x, x') + \underline{A} e^{\gamma_1 |\underline{d}|} K_{zhd}(x, x'), \tag{12}$$

where

$$K_{zh}(x, x') = e^{-\underline{\gamma}_1 r_{zh}}, \;\; r_{zh} = \sqrt{\rho^2 + (z+h)^2}, \tag{13}$$

$$K_{zhd}(x, x') = e^{-\underline{\gamma}_1 r_{zhd}}, \;\; r_{zhd} = \sqrt{\rho^2 + (z+h+|\underline{d}|)^2}. \tag{14}$$

Constants $\underline{B}$, $\underline{A}$ and $\underline{d}$ are evaluated matching $\tilde{T}_{\eta 1}$ and $\tilde{T}^{a}_{\eta 1}$ and their first derivatives at certain characteristic points in the range of integration.

Proposed model - Case 2

Let us assume (9) in the following form

$$\tilde{T}^{a}_{\eta 1} = \underline{B} + \underline{A} e^{-(u_1 \underline{d})}. \tag{15}$$

which gives

$$U^{a}_{11} = \underline{B} K_{zh}(x, x') + \underline{A} K_{zhd}(x, x'). \tag{16}$$

Again, constants $\underline{B}$, $\underline{A}$ and $\underline{d}$ are evaluated matching $\tilde{T}_{\eta 1}$ and $\tilde{T}^{a}_{\eta 1}$ and their first derivatives at certain characteristic points in the range of integration.

Proposed models; Matching points

1. $u_1 \to \infty$, matching point for $\tilde{T}_{\eta 1}$ and $\tilde{T}^a_{\eta 1}$
2. $u_1 = \underline{\gamma}_0$, matching point for $\tilde{T}_{\eta 1}$ and $\tilde{T}^a_{\eta 1}$
3. $u_1 = \underline{\gamma}_0$, matching point for the first derivative of $\tilde{T}_{\eta 1}$ and $\tilde{T}^a_{\eta 1}$

Model	$\underline{B}$	$\underline{A}$	$\underline{d}$
Case 1	1	$\frac{1-\sqrt{2-\underline{n}^2}}{1+\sqrt{2-\underline{n}^2}} e^{\underline{\gamma}_0 \underline{d}(1-\underline{n})}$	$\frac{2}{\underline{\gamma}_0\sqrt{2-\underline{n}^2}}$
Case 2	1	$\frac{1-\sqrt{2-\underline{n}^2}}{1+\sqrt{2-\underline{n}^2}} e^{\underline{\gamma}_0 \underline{d}}$	$\frac{2}{\underline{\gamma}_0\sqrt{2-\underline{n}^2}}$

Table: Obtained values of constants describing proposed models.

Hallén's Integral Equation (HIE)

Boundary condition $\rightarrow$ partial diff. eq. $\rightarrow$ Hallén's IE

$$\int_{-l}^{l} I(x')\,[K_o(x,x') - K_i(x,x') + U_{11}]\,\mathrm{d}x' - C\cos(\mathrm{j}\underline{\gamma}_1 x) = \mathrm{j}\frac{n}{60}U\sin(\mathrm{j}\underline{\gamma}_1 x),$$

where C is an integration constant.

$\rightarrow$ Polynomial current approximation

$$I(u' = x'/l) = \sum_{m=0}^{M} I_m u'^m,\ 0 \le u' \le 1,$$

where I_m, $m = 0,\ 1, ...,\ M$, are complex current coefficients

$\rightarrow$ Point-matching method: $x_i = il/M$, $i = 0,\ 1, ...,\ M$
$I(-l) = I(l) = 0$

Hallén's Integral Equation (HIE)

$$\sum_{m=0}^{M} I_m \int_{-l}^{l} \left(\frac{x'}{l}\right)^m [K_o(x,x') - K_i(x,x') + U_{11}^a(x,x')]\,\mathrm{d}x' - C\cos(\beta_0 \underline{n} x_i) =$$

$$= -\mathrm{j}\frac{\underline{n}}{60} U \sin(\beta_0 \underline{n} x_i),\ \ i = 0,\ 1,\ 2, ...,\ \ M,$$

$$\sum_{m=0}^{M} I_m = 0.$$

Some results

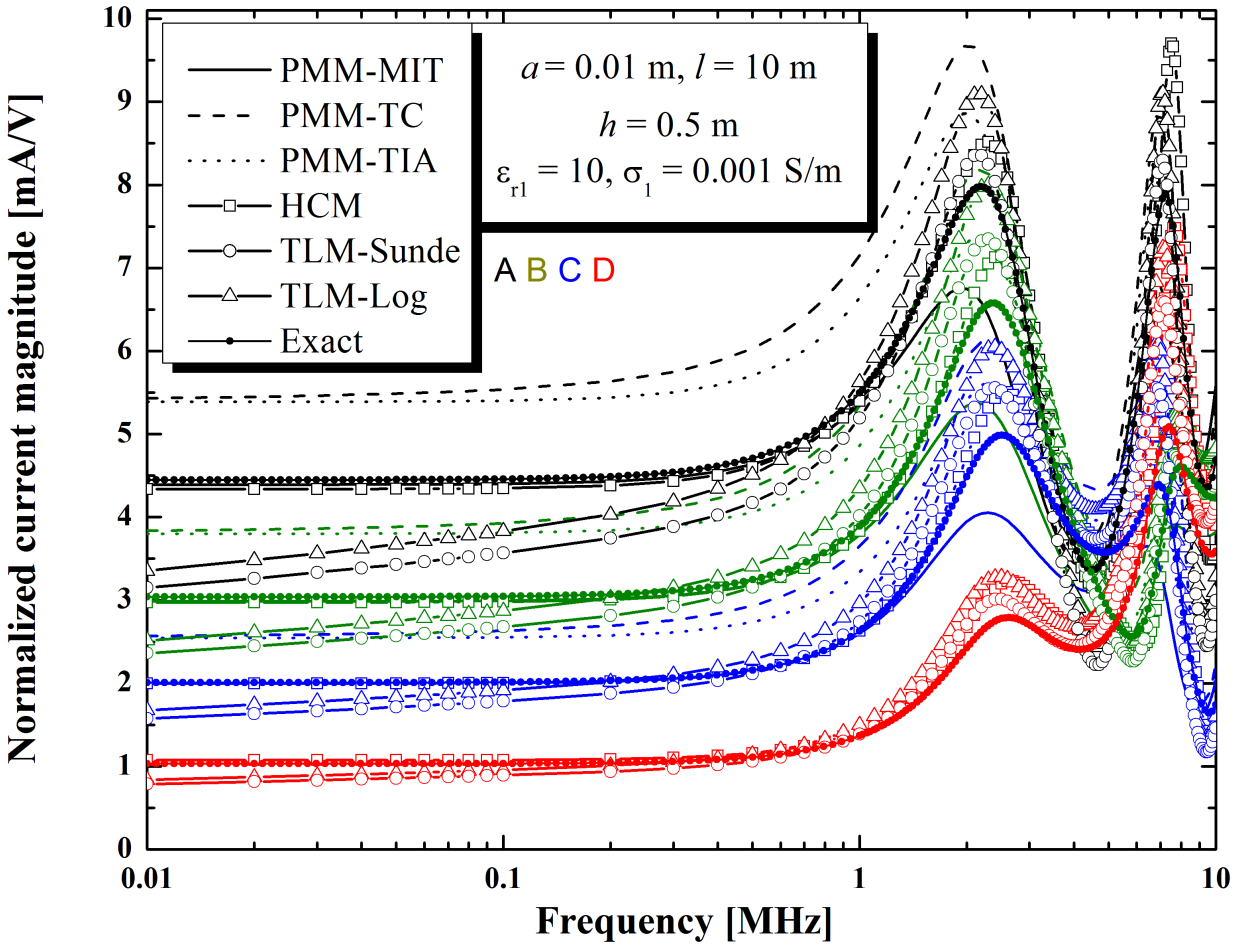

Some results

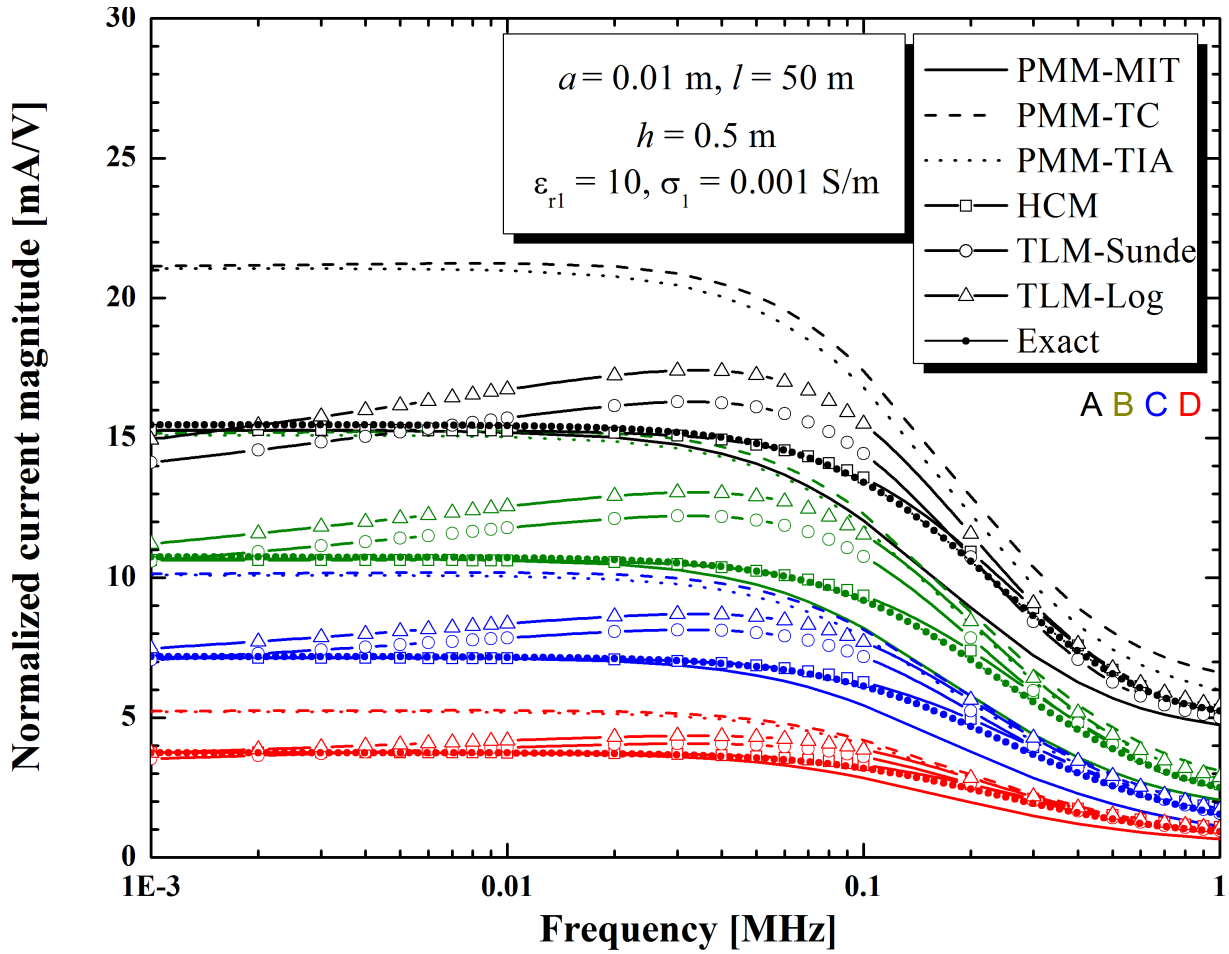

Some results

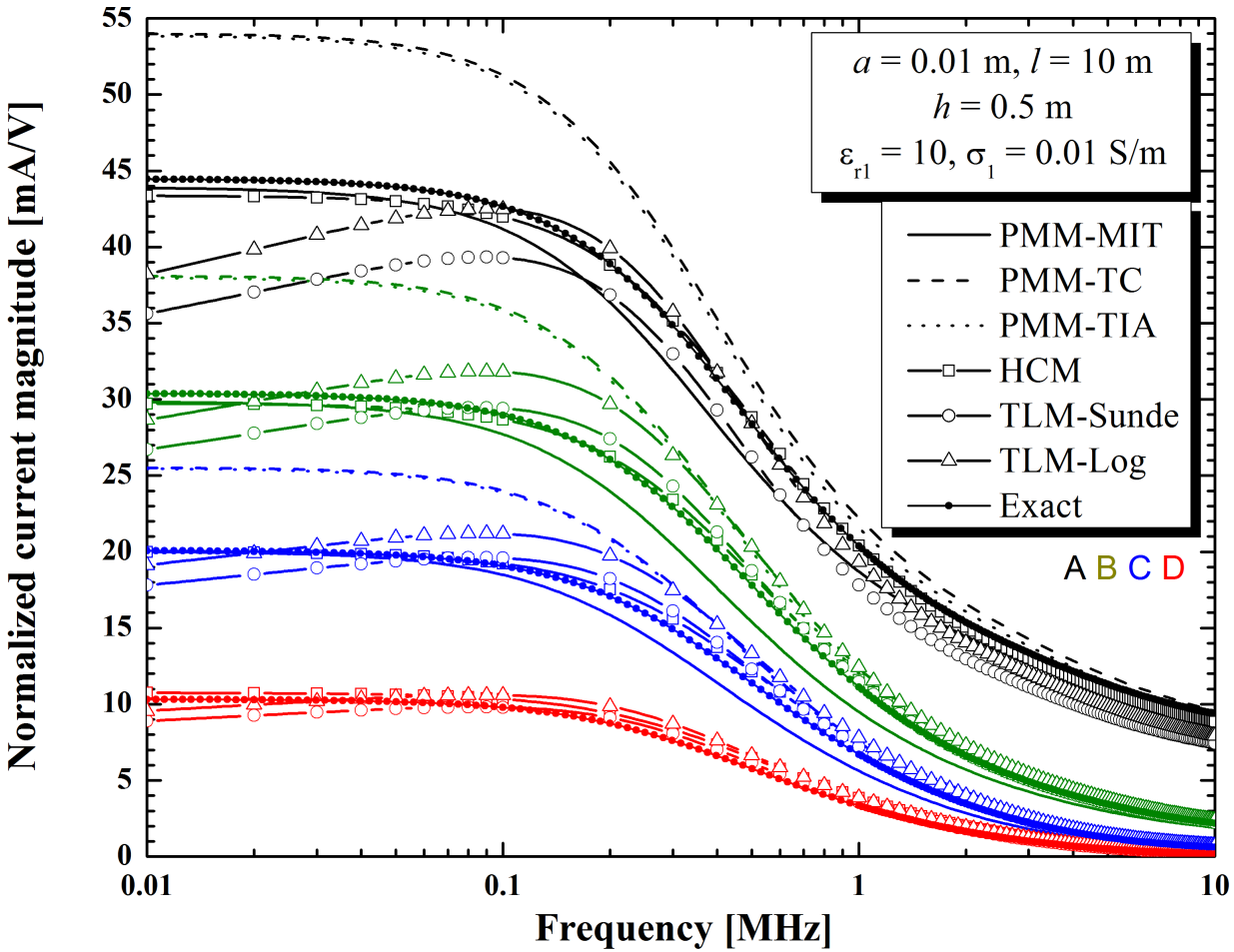

Some results

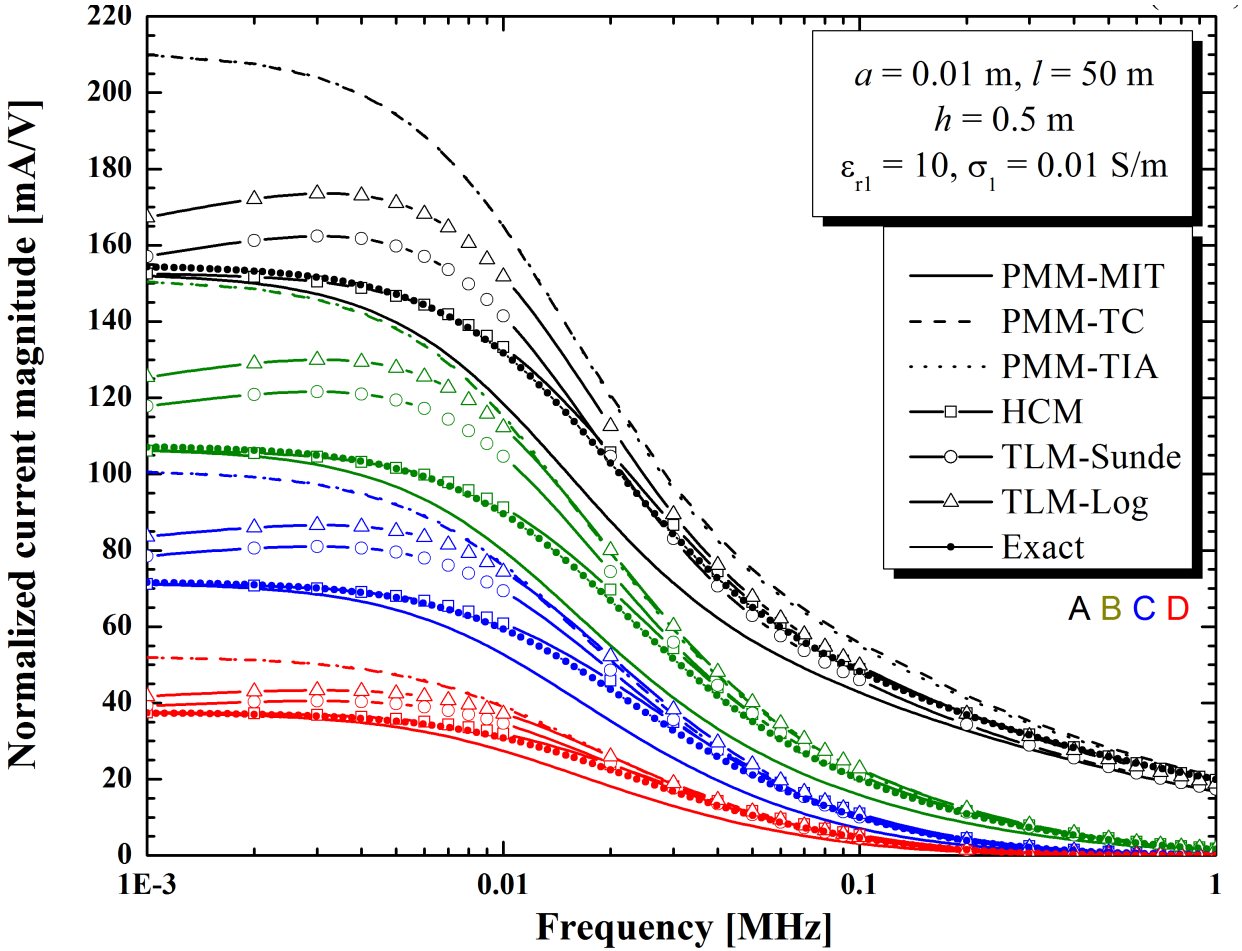

Some results

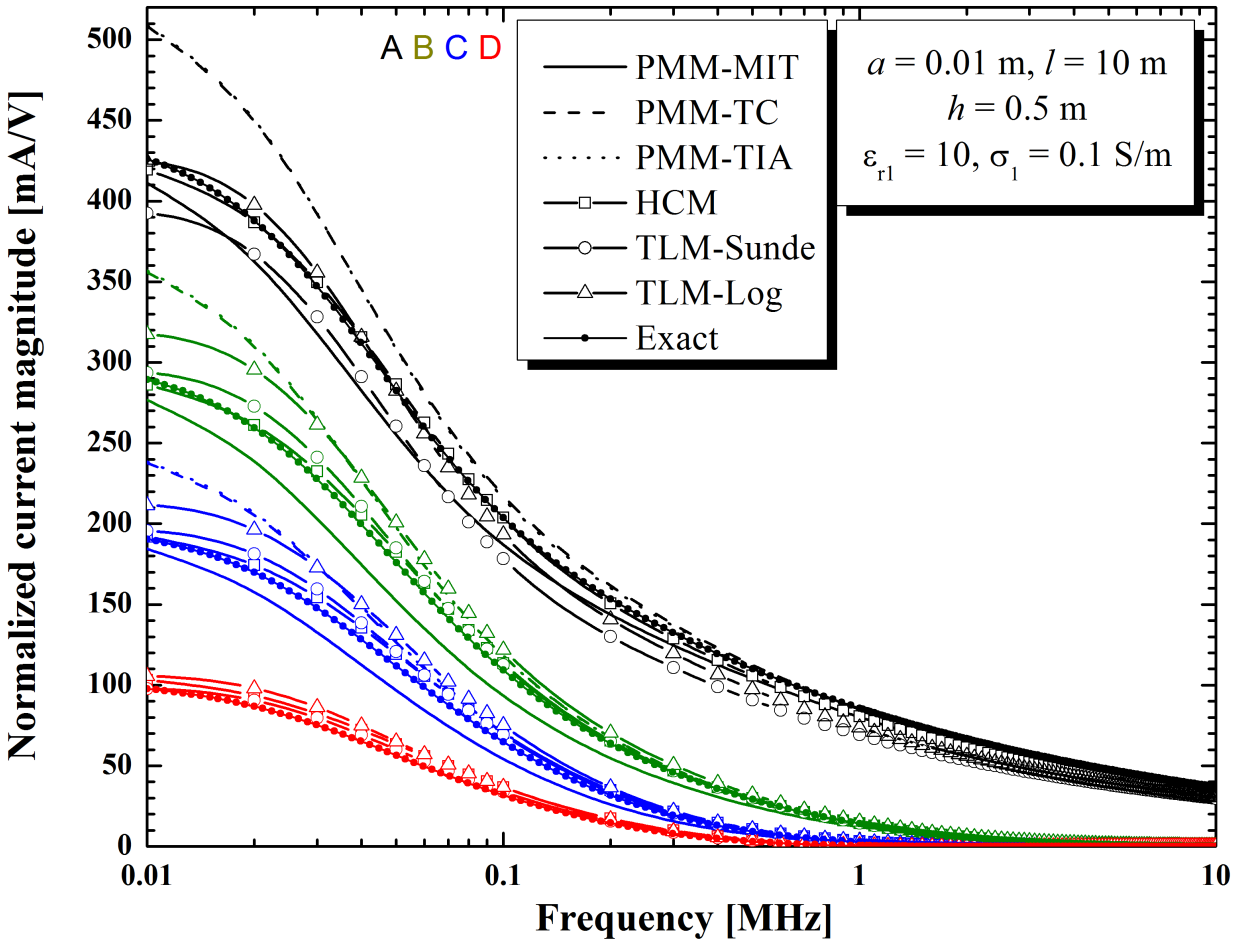

Some results

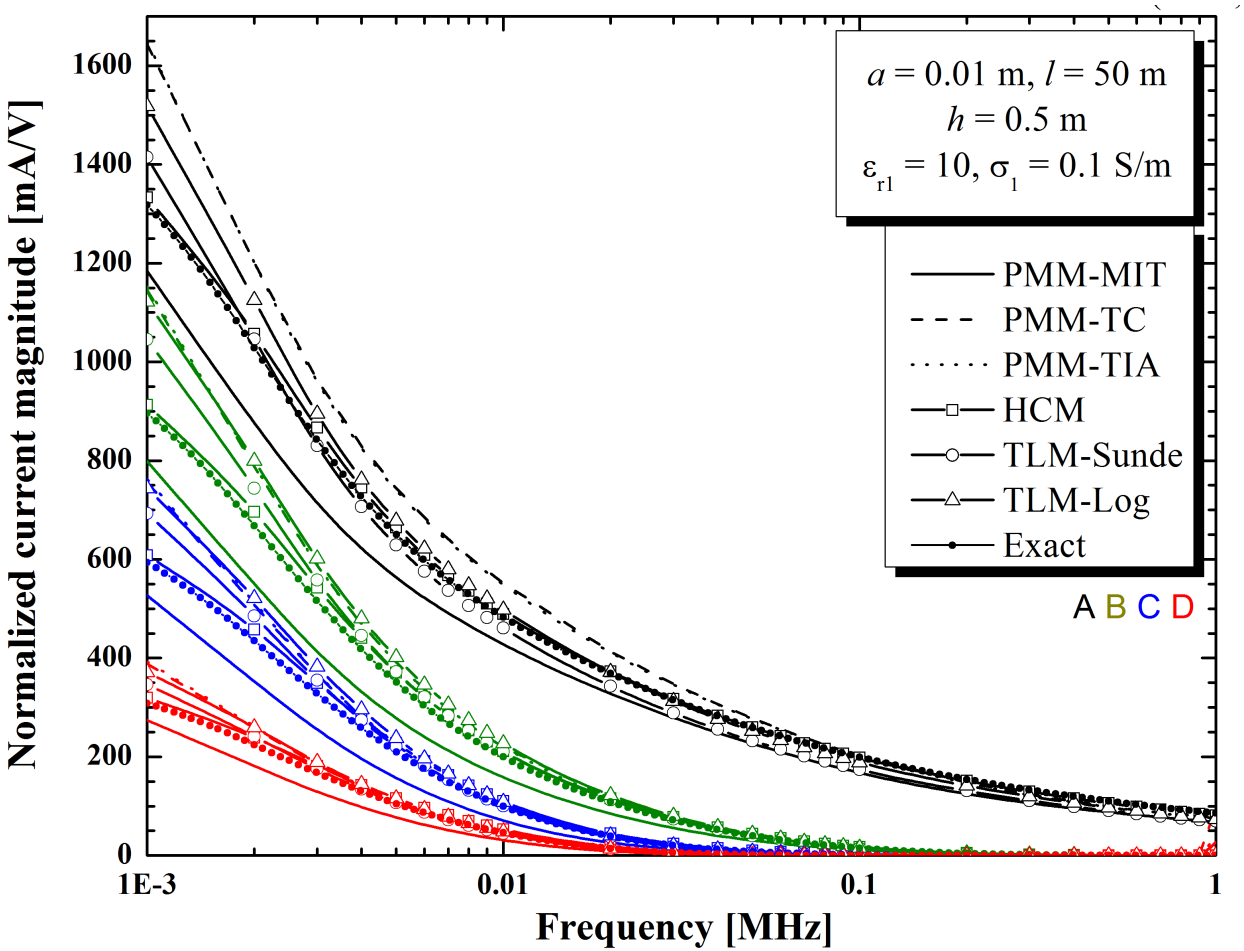

Some results

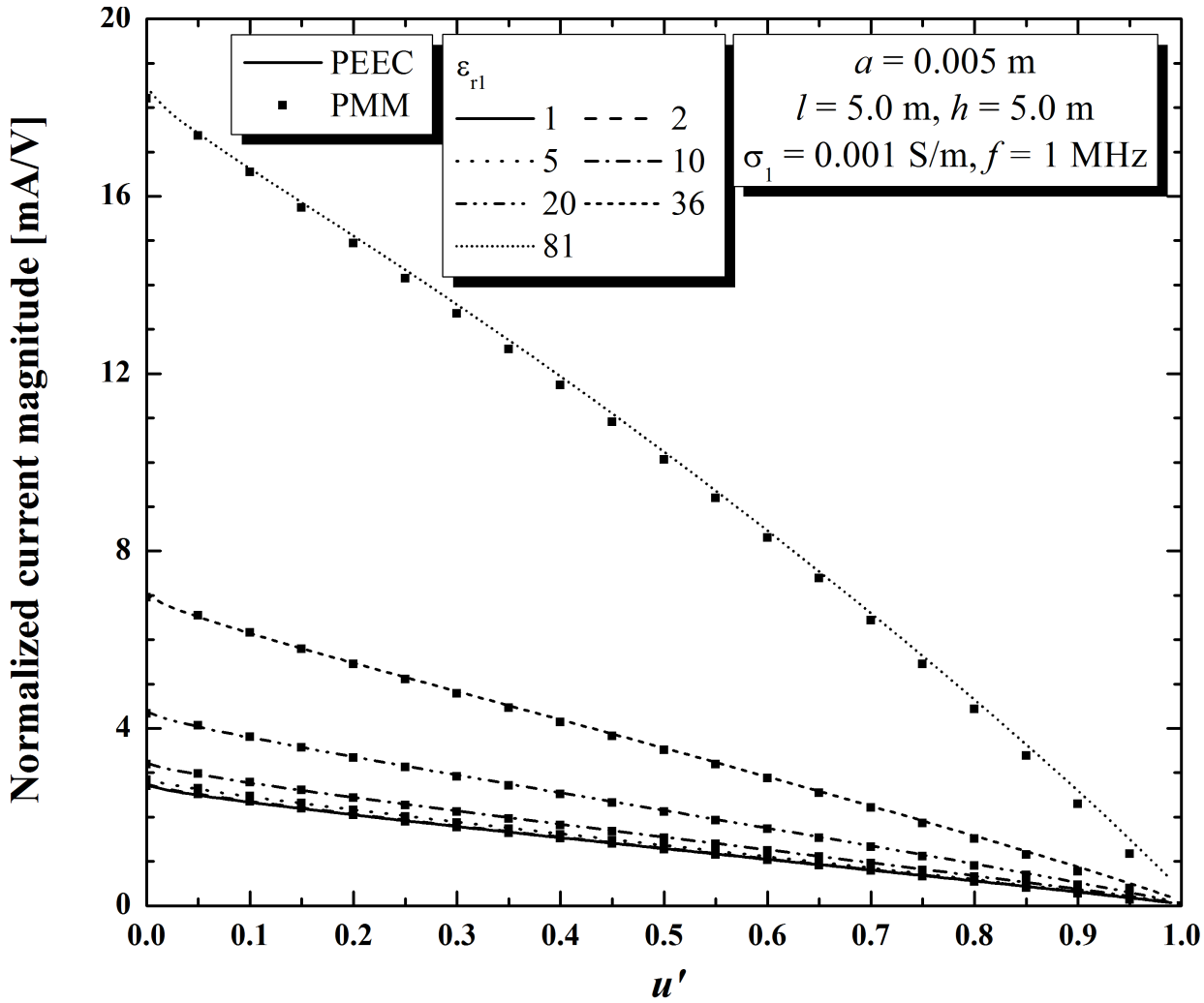

Some results

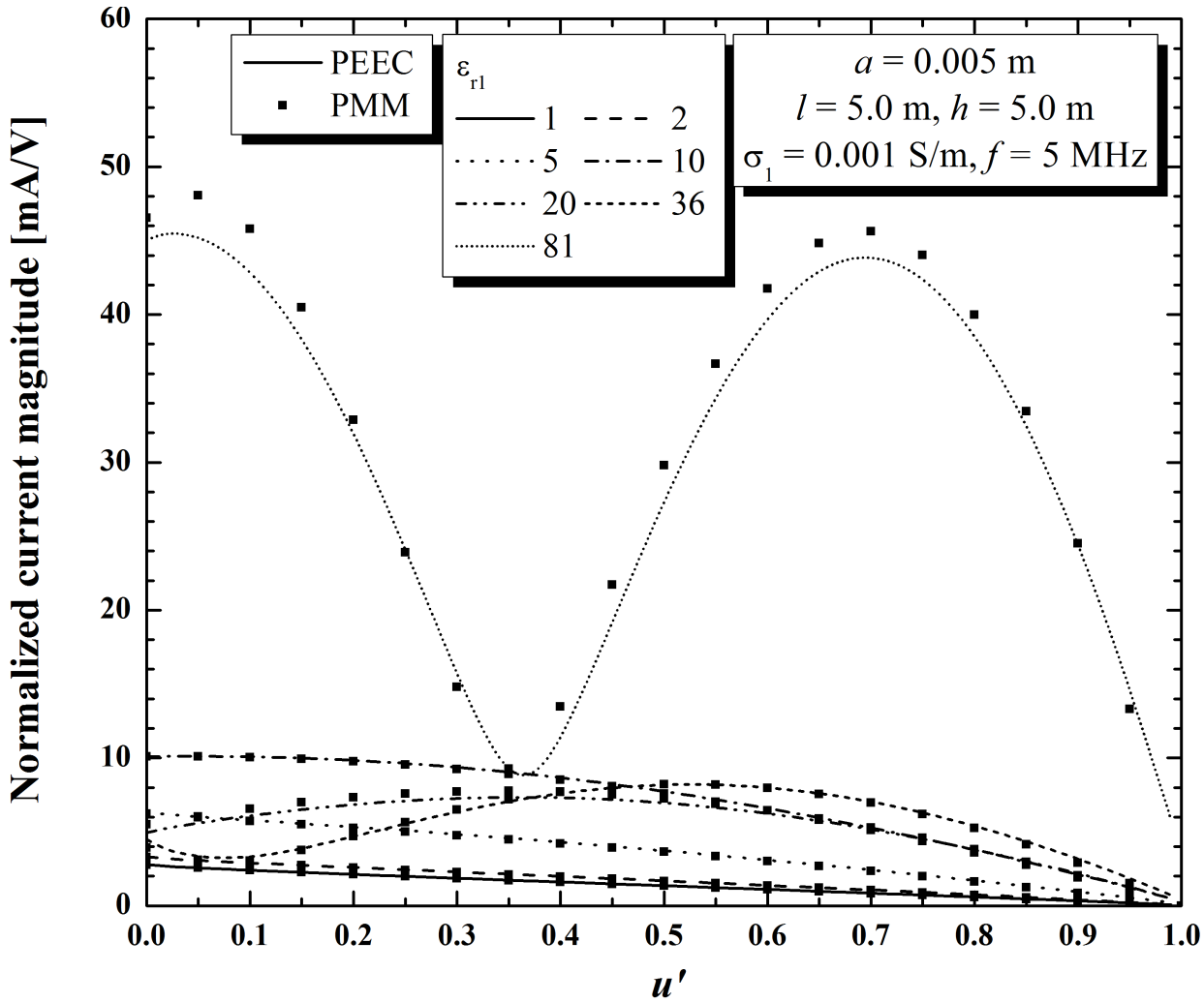

Some results

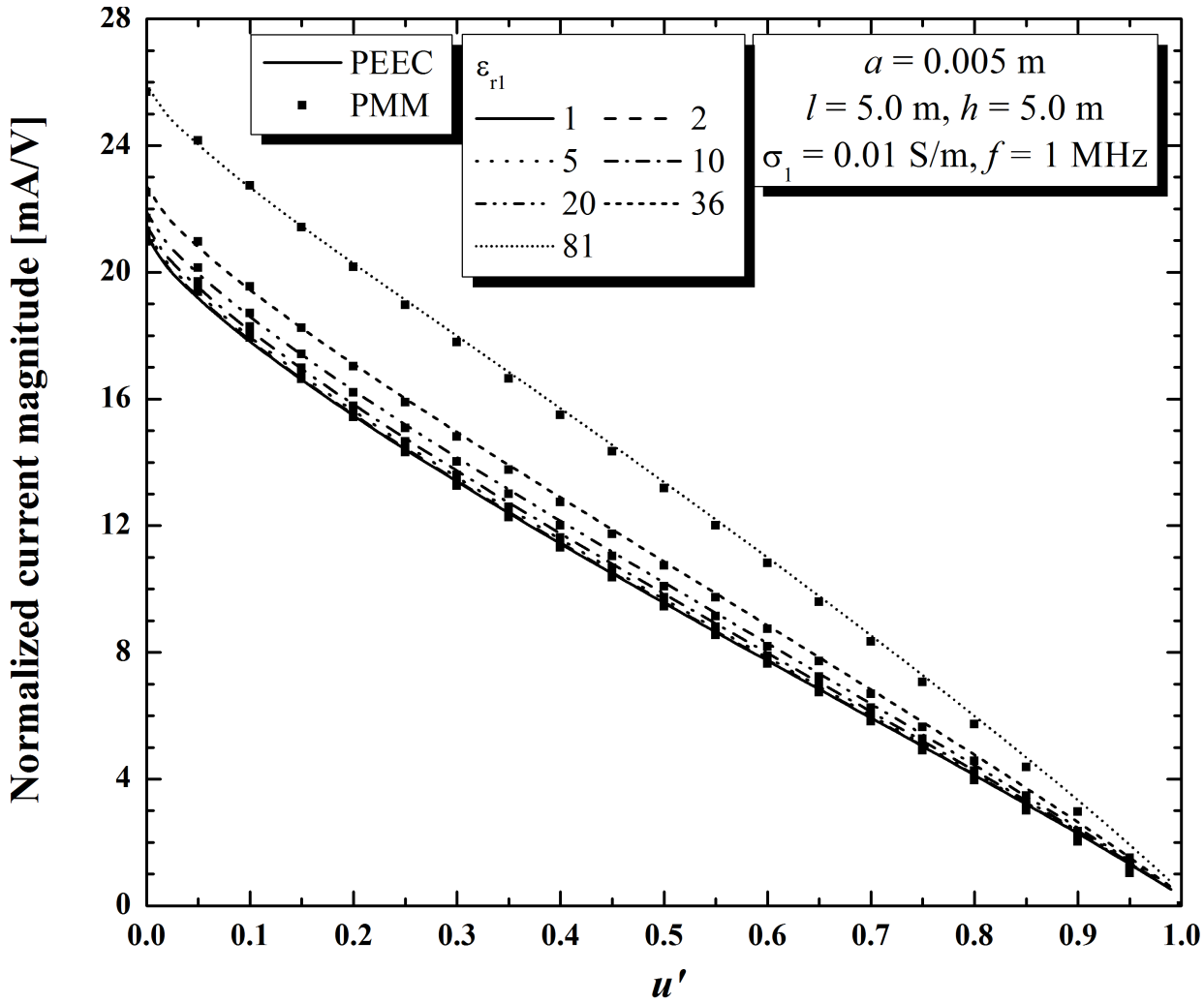

Some results

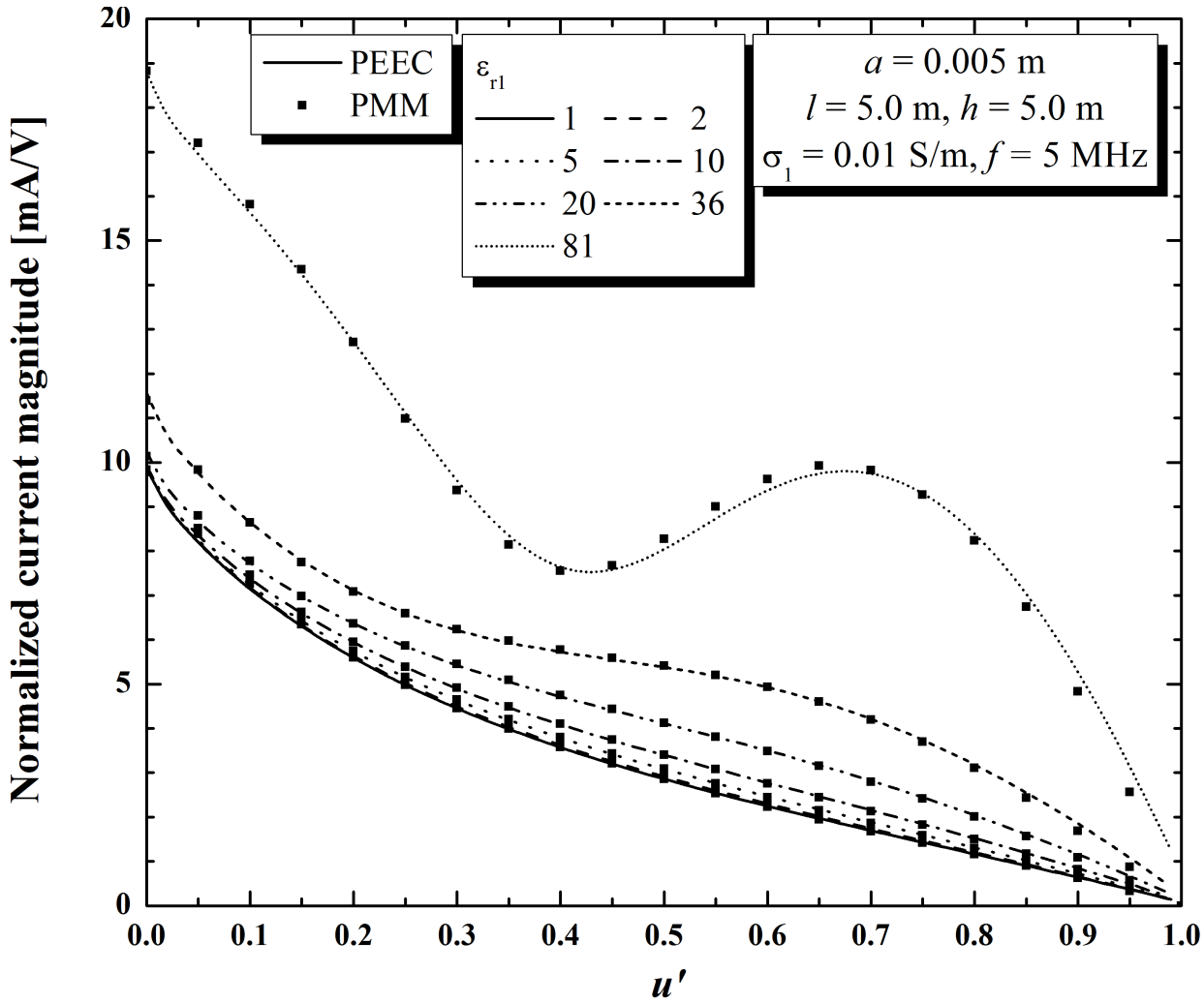

Conclusions

- Proposed approximation behave well in different observed situations, regardless of the electrical properties of the soil, or the position of the source.
- Such characteristics allow these models to be implemented in the analysis of various wire systems buried in the semi-conducting soil (ground electrodes, buried wire antennas, submarine dipoles, buried telecommunication cables, etc.).

Further work

- Presented results indicate a possibility of effective application of the proposed procedure to another form of Sommerfeld integral that also appears in the observed case of sources buried in the semi-conducting ground, which is usually neglected in mentioned analysis.

Sommerfeld integral, 2nd form

$$W_{11} = \int_{\alpha=0}^{\infty} \tilde{T}_{\eta 2}(\alpha) e^{-u_1(z+h)} \frac{\alpha}{u_1} J_0(\alpha\rho) \mathrm{d}\alpha,$$

where

$$\tilde{T}_{\eta 2}(\alpha) = \frac{2u_1(u_1 - u_0)}{\underline{\gamma}_0^2 u_1 + \underline{\gamma}_1^2 u_0}, \quad u_i = \sqrt{\alpha^2 + \underline{\gamma}_i^2}, \quad i = 0, 1,$$

Electrostatic discharges

- An electrostatic discharge (ESD) is a sudden flow of charge from one object to another, often accompanied by an electrical spark.
- Often the charge imbalance is due to a complex phenomenon such as
  - triboelectric charging,
  - electrostatic induction,
  - energetic charged particles colliding with object,
  - ion transfer.
- Most familiar examples of ESDs are probably
  - a) lightning discharges,
  - b) human-to-object discharges.

Modelling of lightning discharge current waveforms

- Objective is to find set of functions that can be used to approximate lightning current waveforms. There have been many such functions proposed, eg. those by Heidler and Cvetic (Heidler 1985,* Heidler and Cvetic), and Javor among others.
- The standard function for approximation is the Heidler wavefunction

$$i(t) = \frac{I_0}{\eta} \frac{\left(\frac{t}{\tau_1}\right)^n}{1 + \left(\frac{t}{\tau_1}\right)^n} e^{-\frac{t}{\tau_2}}$$

or linear combinations thereof.


F. Heidler, "Travelling current source model for LEMP calculation" in *Proceedings of papers, 6th Int. Zurich Symp. EMC, Zurich*, 1985, pp. 157–162.


F. Heidler and J. Cvetic. A class of analytical functions to study the lightning effects associated with the current front, *Transactions on Electrical Power*, 12, 2, 141–150, 2002.

Modelling of lightning discharge current waveforms

- *Downfall of Heidler*: There are no known analytic expressions for the integral of the Heidler function.
- We examine a possible alternative to the Heidler function for approximating waveforms with several 'peaks' that has an analytic expression for its integral.
- Proposed function is defined as a generalized version of the analytically extended function (AEF) suggested by Javor, 2012.

V. Javor. Multi-peaked functions for representation of lightning channel-base currents, *Proceedings of papers, 2012 International Conference on Lightning Protection - ICLP, Vienna, Austria*, 2012, pp. 1–4.

Modelling of the standard ESD current

- Standard ESD from IEC 61000-4-2 (2009).
- Only given a graphical representation and some key parameters.

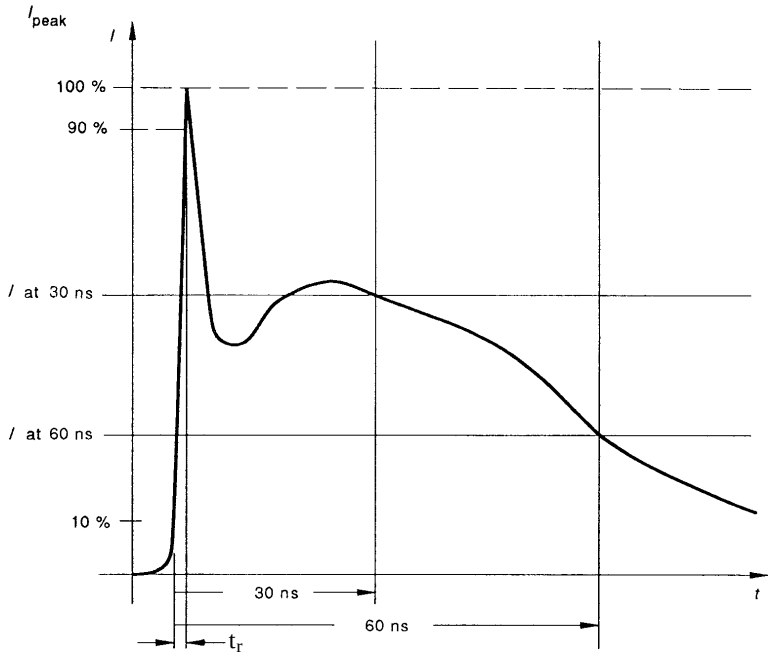

Voltage [kV]	I_{peak} [A]	t_r [ns]	I_{30} [A]	I_{60} [A]
2	$7.5 \pm 15\%$	$0.8 \pm 25\%$	$4.0 \pm 30\%$	$2.0 \pm 30\%$
4	$15.0 \pm 15\%$	$0.8 \pm 25\%$	$8.0 \pm 30\%$	$4.0 \pm 30\%$
6	$22.5 \pm 15\%$	$0.8 \pm 25\%$	$12.0 \pm 30\%$	$6.0 \pm 30\%$
8	$30.0 \pm 15\%$	$0.8 \pm 25\%$	$16.0 \pm 30\%$	$8.0 \pm 30\%$

Modelling of the standard ESD current

- In the literature there are many models for representation of ESD currents, either the IEC 61000-4-2 Standard one [1], or experimentally measured ones.
- They have to satisfy the following:
  - the value of the ESD current and its first derivative must be equal to zero at moment $t = 0$, since neither the transient current nor the radiated field generated by the ESD current can change abruptly at that moment.
  - the ESD current function must be time-integrable in order to allow numerical calculation of the ESD radiated fields.
- There have been many different models proposed for the Standard ESD, we will examine approximation using a model called the *Analytically Extended Function* (AEF).

Functions for ESD current modelling

- Double exponential, Cerri *et al.* (1996)

$$i(t) = I_1 e^{-\frac{t}{\tau_1}} - I_2 e^{-\frac{t}{\tau_2}}$$

- Four - exponential function, Keenan and Rosi (1991)

$$i(t) = I_1 \left[e^{-\frac{t}{\tau_1}} - e^{-\frac{t}{\tau_2}} \right] - I_2 \left[e^{-\frac{t}{\tau_3}} - e^{-\frac{t}{\tau_4}} \right]$$


G. Cerri, R. Leo, V. M. Primiani. ESD Indirect Coupling Modelling. *IEEE Trans. on EMC*, Vol. 38, pp. 274-281, 1996.


R. K. Keenan, L. K. A. Rossi. "Some fundamental aspects of ESD testing", in *Proc. IEEE Int. Symp. on Electromagnetic Compatibility*, Aug. 12-16, 1991, pp. 236-241.

Functions for ESD current modelling

- Pulse function, Feizhou and Shange (2002)

$$i(t) = I_0 \left[1 - e^{-\frac{t}{\tau_1}}\right]^p e^{-\frac{t}{\tau_2}}$$

and its extensions

- binomial, Songlin *et al.*(2003)

$$i(t) = I_0 \left[1 - e^{-\frac{t}{\tau_1}}\right]^p e^{-\frac{t}{\tau_2}} + I_1 \left[1 - e^{-\frac{t}{\tau_3}}\right]^q e^{-\frac{t}{\tau_4}}$$

- trinomial and quadrinomial, Yuan *et al.* (2006)


Z. Feizhou, L. Shange. A new function to represent the lightning return-stroke currents. *IEEE Trans. on EMC*, Vol. 44, pp. 595-597, 2002.


S. Songlin, B. Zengjun, T. Minghong, L. Shange, A new analytical expression of current waveform in standard IEC61000-4-2. *High Power Laser and Particle Beams*, No.5, pp. 464-466, 2003.


Z. Yuan, T. Li, J. He, S. Chen, R. Zeng. New mathematical descriptions of ESD current waveform based on the polynomial of pulse function. *IEEE Transactions on EMC*, Vol.48, No.3, pp. 589-591, 2006.

Functions for ESD current modelling, cont'd...

- Based on the Heidler function, Heidler (1985)

$$i(t) = \frac{I_0}{\eta} \frac{\left(\frac{t}{\tau_1}\right)^n}{1 + \left(\frac{t}{\tau_1}\right)^n} e^{-\frac{t}{\tau_2}}$$

Wang *et al.* (2003) propose double Heidler

$$i(t) = \frac{I_1}{\eta_1} \frac{\left(\frac{t}{\tau_1}\right)^n}{1 + \left(\frac{t}{\tau_1}\right)^n} e^{-\frac{t}{\tau_2}} + \frac{I_2}{\eta_2} \frac{\left(\frac{t}{\tau_3}\right)^n}{1 + \left(\frac{t}{\tau_3}\right)^n} e^{-\frac{t}{\tau_4}}$$


F. Heidler, "Travelling current source model for LEMP calculation", in *Proceedings of papers, 6th Int. Zurich Symp. EMC, Zurich*, 1985, pp. 157–162.


K. Wang, D. Pommerenke, R. Chundru, T. Van Doren, J. L. Drewniak, A. Shashindranath. Numerical modeling of electrostatic discharge generators. *IEEE Transactions on EMC*, Vol.45, No.2, pp. 258-271, 2003.

Functions for ESD current modelling, cont'd...

- Gaussian based function, Berghe and Zutter, (1998)

$$i(t) = Ae^{-\left(\frac{t-t_1}{\sigma_1}\right)^2} + Bte^{-\left(\frac{t-t_2}{\sigma_2}\right)^2}$$

- Wang *et al.* (2012), propose the following

$$i(t) = Ate^{-Ct} + Bte^{-Dt}$$


S. V. Berghe, D. Zutter. Study of ESD signal entry through coaxial cable shields. *J. Electrostat.*, No.44, pp. 135-148, 1998.


K. Wang, J. Wang, X. Wang. Four order electrostatic discharge circuit model and its simulation. *TELKOMNIKA*, Vol.10, No.8, pp. 2006-2012, 2012.

Models for lightning or ESD current approximation

- Approximation models are typically constructed as linear combinations of functions that share some qualitative properties with the lightning or ESD waveshape (e.g. steep rise and slow decay).
- Javor introduced the AEF for lightning (2012) and ESD currents (2014) and it has been used to approximate various currents, primarily lightning discharges, see for example Lundengård et all, 2016.
- The AEF model is based on piecewise linear combinations of *power exponential functions*.


V. Javor. Multi-peaked functions for representation of lightning channel-base currents, *Proceedings of papers, 2012 International Conference on Lightning Protection - ICLP, Vienna, Austria*, 2012, pp. 1–4.


V. Javor, "New function for representing IEC 61000-4-2 standard electrostatic discharge current," Facta Universitatis, Series: Electronics and Energetics, vol. 27(4), pp. 509–520, 2014.


K. Lundengård, M. Rančić, V. Javor, and S. Silvestrov, "Estimation of parameters for the multi-peaked AEF current functions," Methodol. Comp. Appl. Probab., pp. 1–15, 2016.

Power exponential function

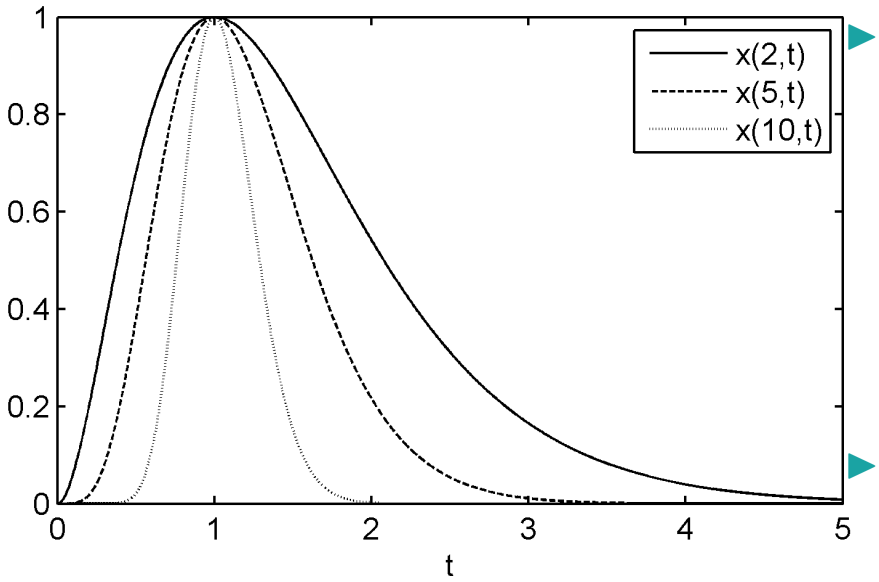

- We will build the approximation from what we call the power exponential function

$$x(\beta; t) = \left(te^{1-t}\right)^{\beta}, \ 0 \leq t.$$

- The steepness of the function increases as β increases.

- Qualitatively similar to other functions that are popular for approximation of ESD phenomena, e.g. the Heidler function, Pulse function and the biexponential function (also popular in other fields such as pharmacokinetics).
- Has been used to model the attack rate of predatory fish.

Power exponential function, *cont'd*

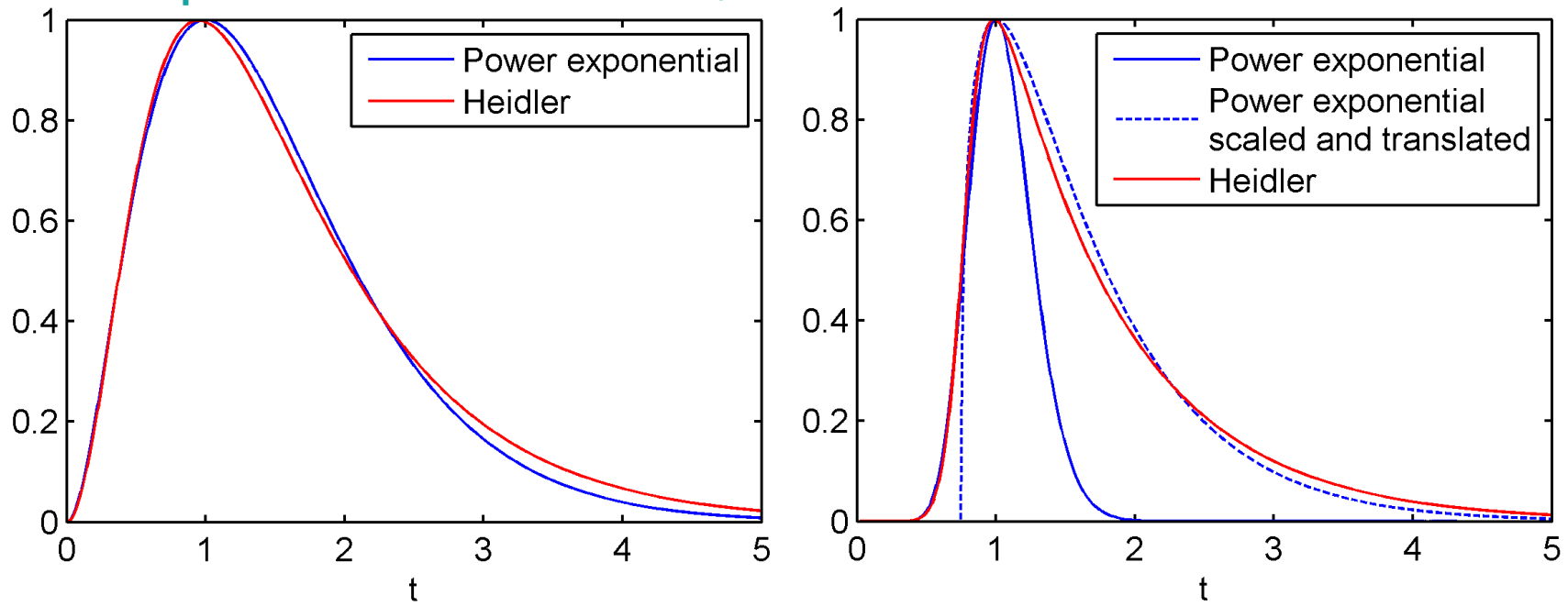

- The approximation in our case consists of piecewise power exponential functions so that the steepness of rise or decay can be controlled locally.
- Scaling and translation of $x(\beta_1, t)$, $t \in [0, 1]$ for rising part and $x(\beta_2, t)$, $t > 1$ for decaying part.

The p-peaked AEF

Let $I_{m_q} \in \mathbb{R}$, $t_{m_q} \in \mathbb{R}$, $q = 1, 2, \ldots, p$, $t_{m_0} = 0 < t_{m_1} < t_{m_2} < \ldots < t_{m_p}$ along with $\eta_{q,k}$, $\beta_{q,k} \in \mathbb{R}$ and $0 < n_q \in \mathbb{Z}$ for $q = 1, 2, \ldots, p+1$, $k = 1, 2, \ldots, n_q$ such that $\sum_{k=1}^{n_q} \eta_{q,k} = 1$.

The *analytically extended function* (AEF), $i(t)$, with p peaks is defined as

$$i(t) = \begin{cases} \left(\sum_{k=1}^{q-1} I_{m_k} \right) + I_{m_q} \sum_{k=1}^{n_q} \eta_{q,k} x_q(t)^{\beta_{q,k}^2+1}, & t_{m_{q-1}} \le t \le t_{m_q},\ 1 \le q \le p, \\ \left(\sum_{k=1}^{p} I_{m_k} \right) \sum_{k=1}^{n_{p+1}} \eta_{p+1,k} x_{p+1}(t)^{\beta_{p+1,k}^2}, & t_{m_p} \le t, \end{cases}$$

where $x_q(t) = \dfrac{t - t_{m_{q-1}}}{\Delta t_{m_q}} \exp\left(\dfrac{t_{m_q} - t}{\Delta t_{m_q}} \right)$, $1 \le q \le p$,

$x_{p+1}(t) = \dfrac{t}{t_{m_q}} \exp\left(1 - \dfrac{t}{t_{m_q}} \right)$ and $\Delta t_{m_q} = t_{m_q} - t_{m_{q-1}}$.

Examples of a 2-peak AEF

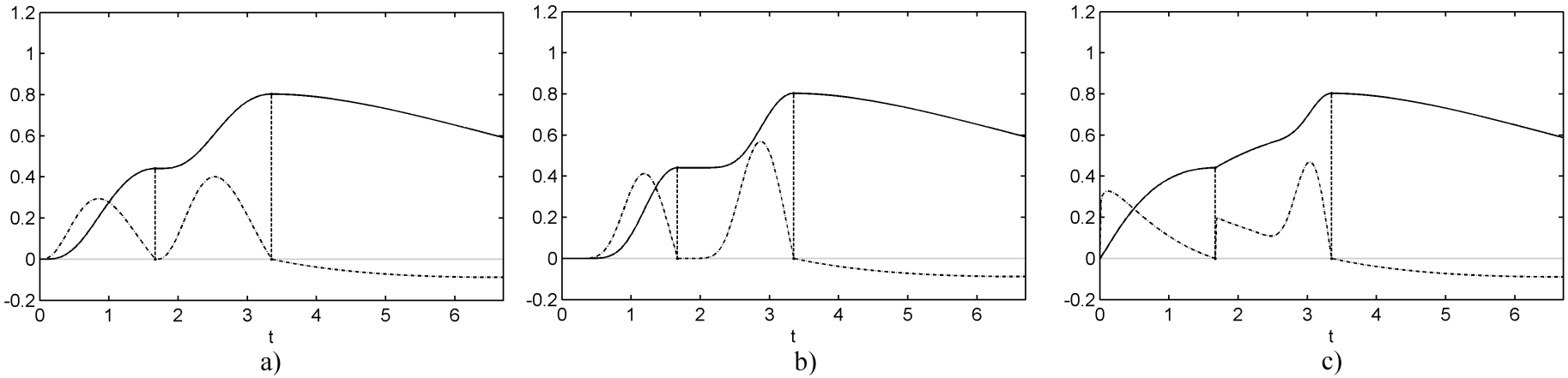

Figure: AEF (solid line) and its derivative (dashed line) with the same I_{m_q} and t_{m_q} but different $\beta_{q,k}$-parameters. (a) $4 < \beta_{q,k} < 5$, (b) $12 < \beta_{q,k} < 13$, (c) a mixture of large and small $\beta_{q,k}$-parameters.

- The AEF and its derivative is continuous since $\beta^2 + 1 \geq 1$.
- The integral of the AEF can be given analytically using the Gamma function, a well-known special function with many known analytical properties that can also be computed fairly efficiently.

Approximation using the AEF

- For simplicity we will consider the scenario where we want to approximate a set of data points (t_k, i_k), $k = 1, 2, \ldots, m$, with a linear combination of $n \leq m$ power-exponential functions.
- The regression model is $i_k = \sum_{j=1}^{n} \eta_j (t_k e^{1-t_k})^{\beta_j} + \epsilon_k$ where ϵ_k is normally distributed random noise.
- The regression model has $2n$ undetermined parameters, η_j and β_j for $j = 1, 2, \ldots, n$.

Estimation of η and β parameters

- Since the model is linear in η and non-linear in β we can use a combination of methods to find all parameters even when $n \leq m < 2n$.
- For finding the β parameters we will use the Marquardt least-squares method (MLSM), a well-known iterative numerical method for solving non-linear regression problems.
- for finding the η parameters we will use the regular least-squares method for linear models.
- For a detailed description of the fitting procedure, see [3].

Results for first negative impulse

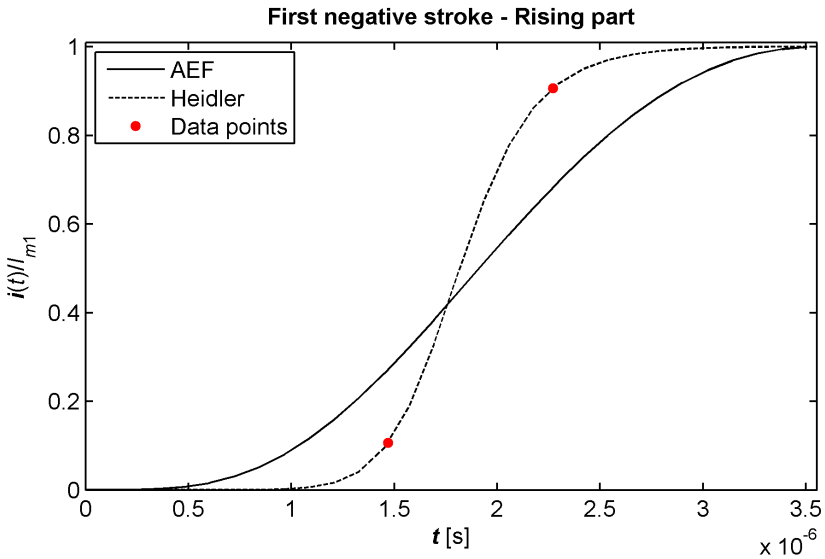

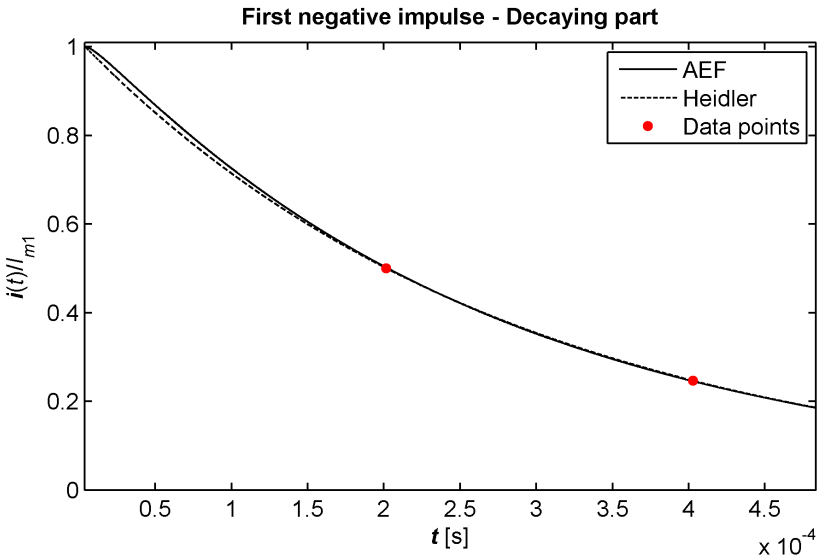

Least-square fitting of the AEF to the first negative impulse, the figure on the right with the condition $0 \leq \eta_{1,k} \leq 1,\ k = 1, 2$.

Results for the first positive stroke

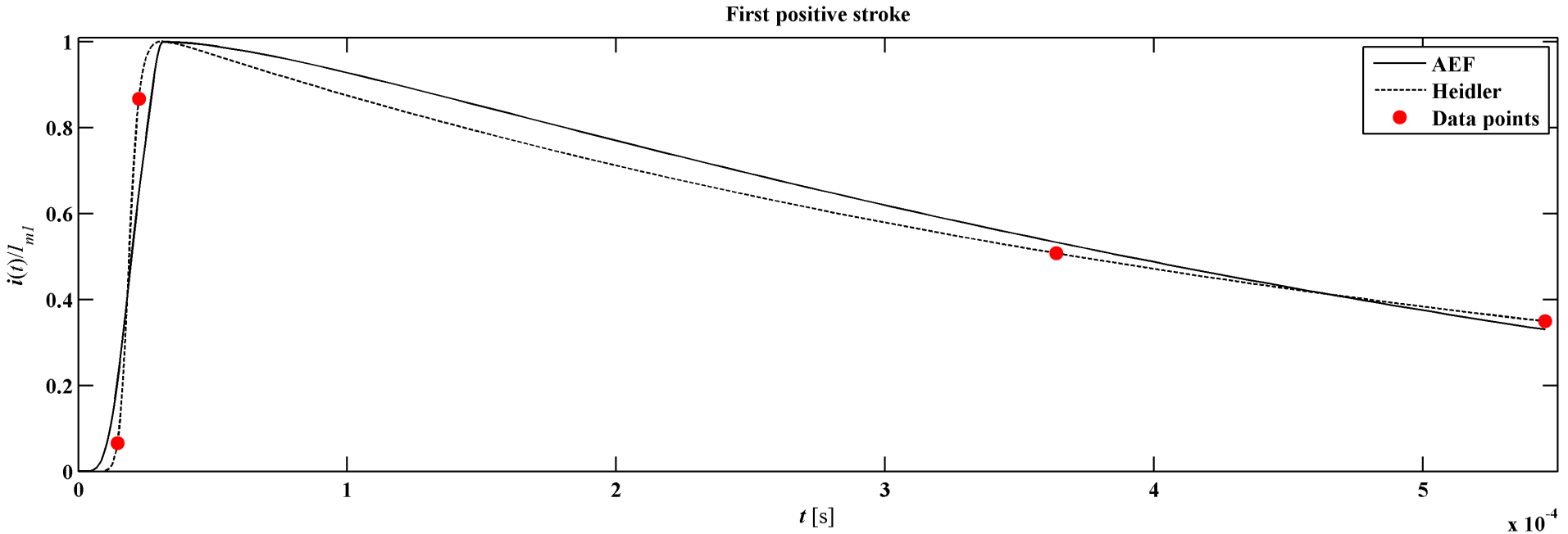

Least-square fitting of the AEF to the first positive stroke. Here the charge transfer and specific energy is also taken into account.

Results for a 2-peaked waveform

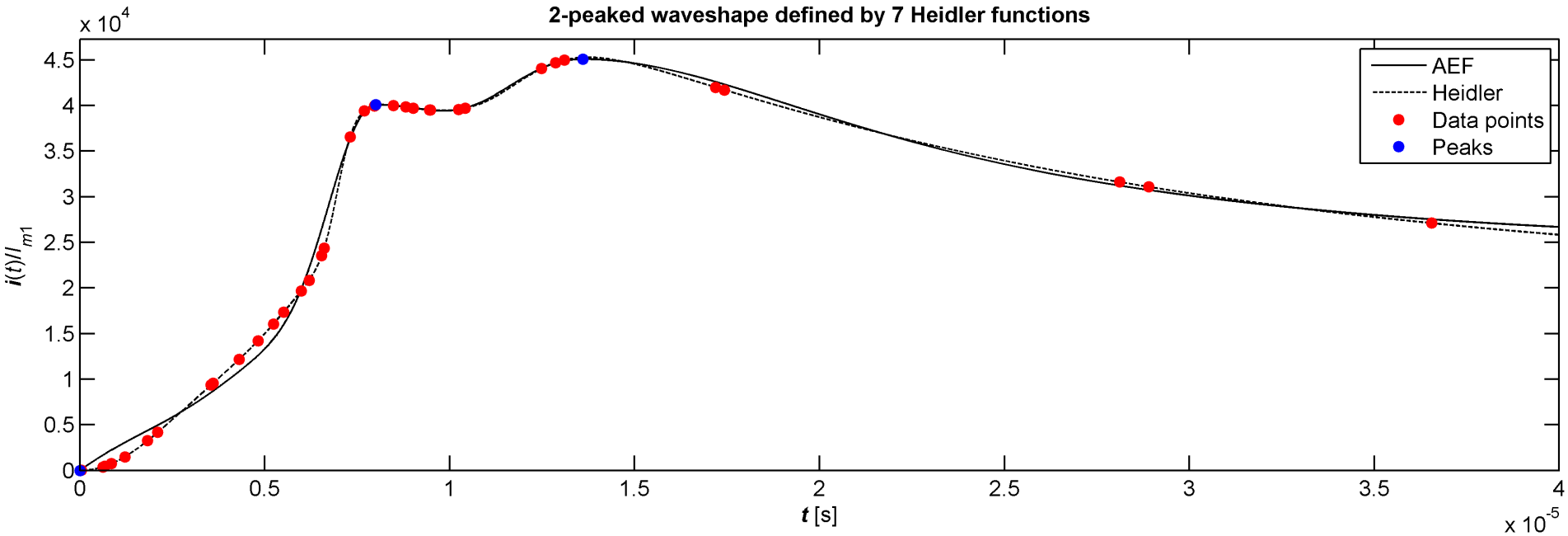

Least-square fitting of an AEF with 3 terms in each interval to a 2-peaked waveform given by a linear combination of 7 Heidler functions Silveira *et. al.*, 2010. Data points were chosen randomly.

F. H. Silveira, A. De Conti and S. Visacro. Lightning Overvoltage Due to First Strokes Considering a Realistic Current Representation, *IEEE Transactions on electromagnetic compatibility*, vol. 52, no. 4, 2010.

Results for a 2-peaked waveform

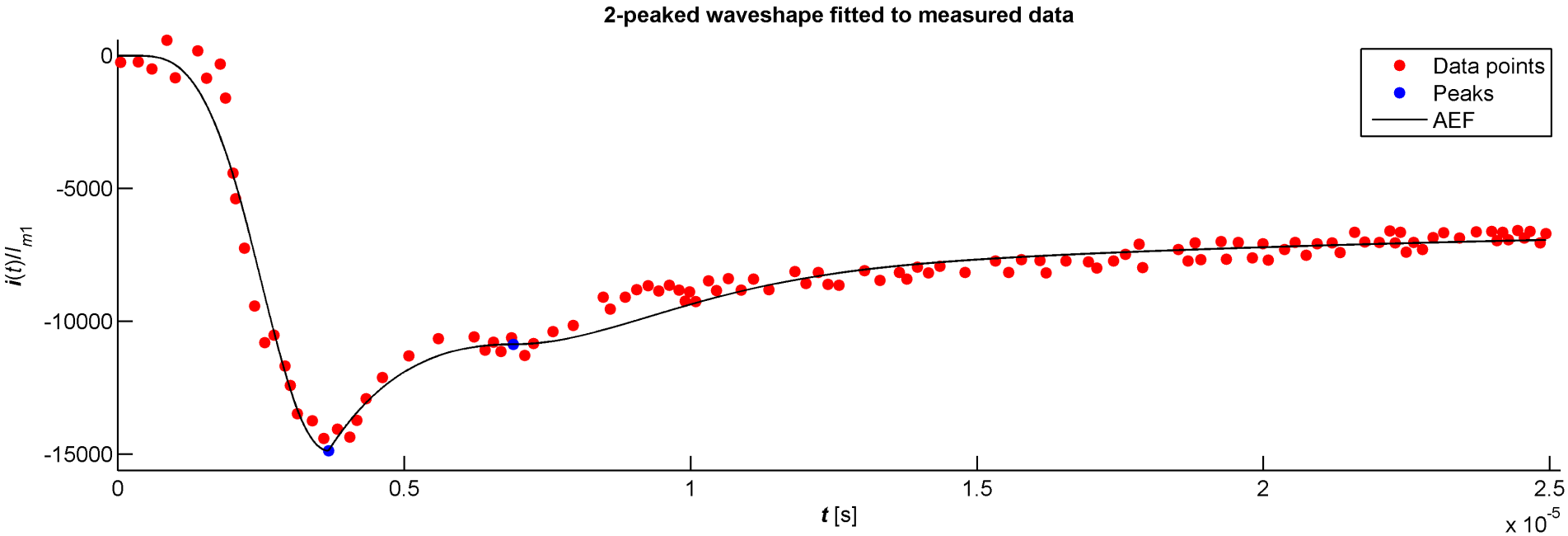

Least-square fitting of an AEF with 2 peaks and 2, 1 and 4 terms in the respective interval to experimental measurements from Berger *et. al.*, 1975

K. Berger, R. B. Anderson and H. Kroninger, Parameters of lightning flashes, *Electra*, vol. 41, pp. 23-37, 1975.

Results for the Standard ESD current

- Below we illustrate the result of fitting various models to the Standard ESD current waveshape for 4kV.

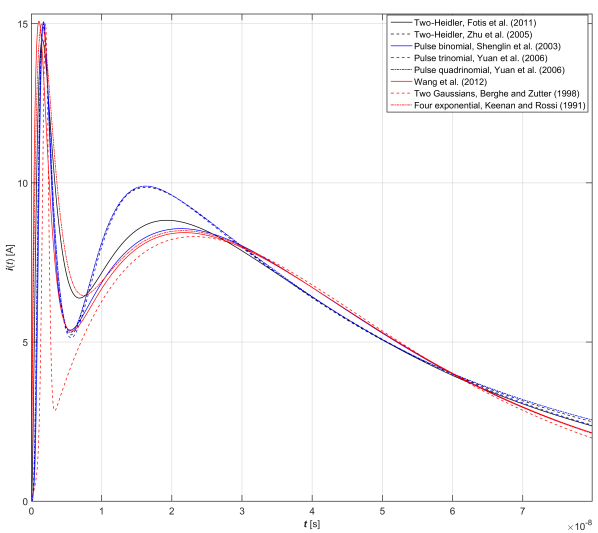

Various models

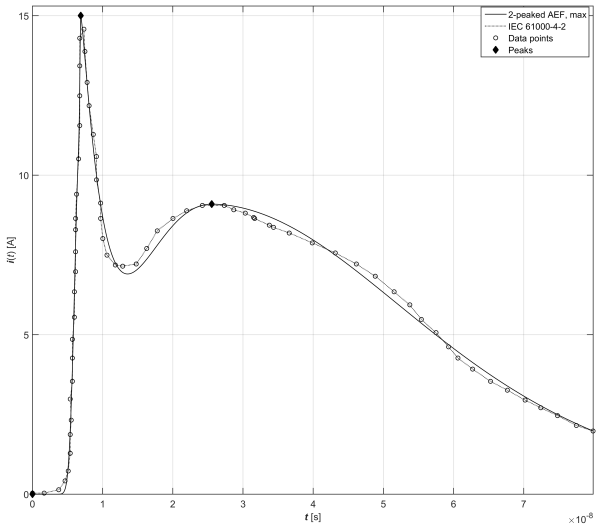

AEF (2,2,2)

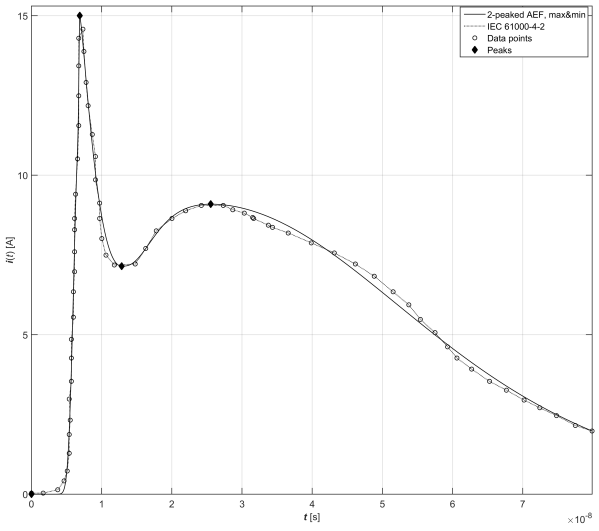

AEF (2,1,2,2)

EMC - Part 4-2: Testing and Measurement Techniques - Electrostatic Discharge Immunity Test. IEC International Standard 61000-4-2, basic EMC publication, Ed. 2, 2009.

Results for a measured ESD current

- Fitting AEF models to measured ESD current from Katsivelis et al, 2010.

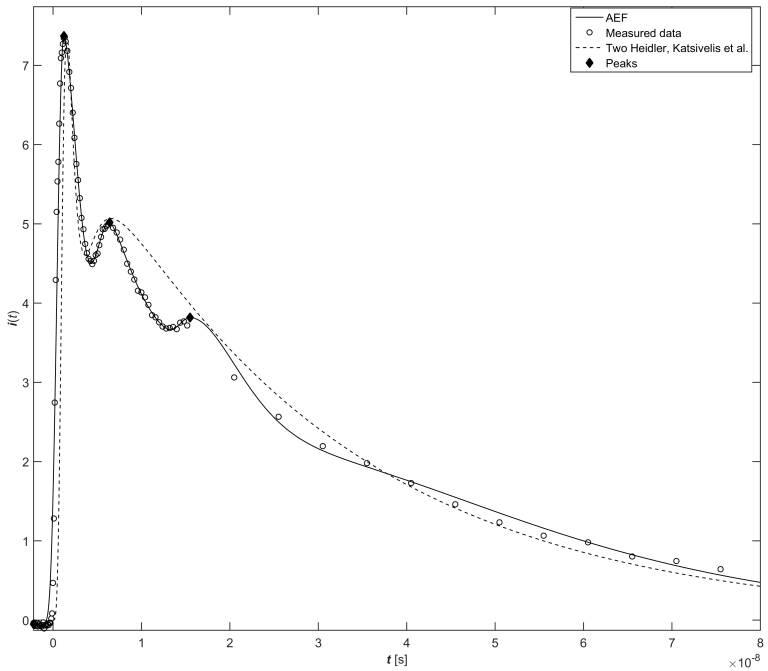

AEF (1,2,2,3)

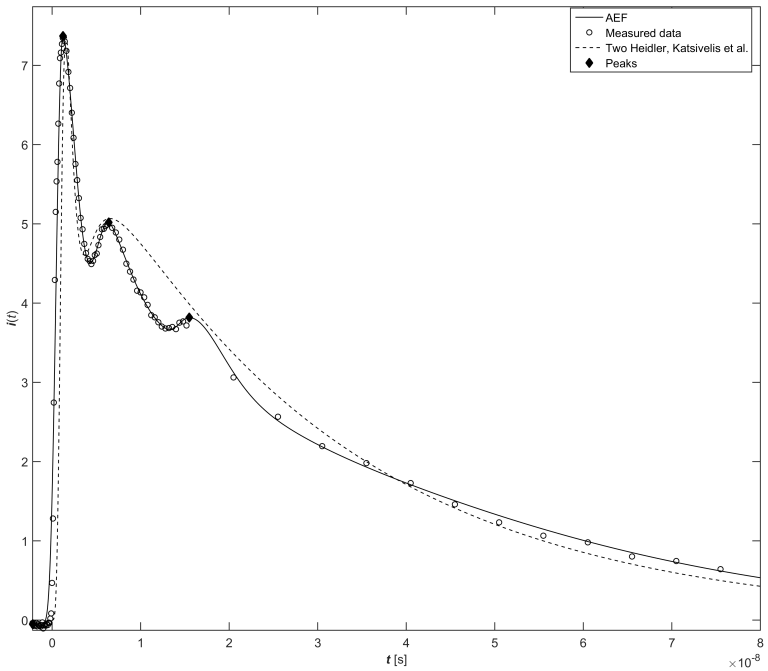

AEF (1,2,2,4)

P. S. Katsivelis, I. F. Gonos, and I. A. Stathopulos, "Estimation of parameters for the electrostatic discharge current equation with real human discharge events reference using genetic algorithms," Meas. Sci. Technol., vol. 21, pp. 1–6, 2010.

Summary

- A mathematical model for representation of multi-peaked lightning and ESD currents presented - the *multi-peaked analytically extended function (AEF)*.
- The AEF function itself and its first derivative are equal to zero at moment $t = 0$, and is time-integrable using a simple special function, and therefore suitable for describing different lightning and ESD current waveforms.
- The AEF can be adjusted to fit desired waveshapes from standards or the ones corresponding to experimentally measured data, using for example the Marquardt least-squares method (MLSM).

Summary, *cont'd*

- The accuracy of the fitting to the reference waveshape depends on the number of terms chosen in the respective time interval and can usually can be improved by increasing this number in the troubled segments.
- Often a good fit can be achieved using relatively few parameters. The current formulation requires some manual choice of peaks times.
- Considering the results of performed numerical experiments, the AEF function should be considered as an alternative analytical expression for representation of multi-peaked lightning and ESD current waveshapes as a part of future editions of corresponding standards.

Further work

- It has been observed that the distribution and number of data points chosen for the optimization procedure also influences the fitting, so finding strategies for sampling the available data should be further investigated. First results were presented at the EMC2017 conference in Washington, USA.
- The used fitting procedure becomes expensive for large amounts of data, it might be necessary to consider alternative methods for fitting.
- Further testing of the model in applications. Do the models properties facilitate the use of common analytical and numerical techniques?

History

- First life insurances in 18th century
- 1725 de Moivre transformation of life tables to simple mathematical laws
- Mortality pattern. Three parts can be observed:
  - Infant mortality
  - " Accident hump"
  - Senescent death

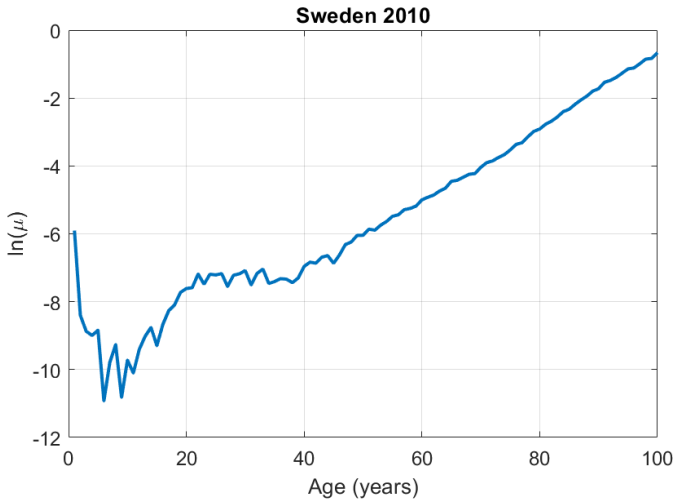

Survival Function

Definition 1 Survival Function

$$S_x(t) = 1 - F_x(t) = \mathrm{P}\{T_x > 1\}$$

Theorem 1

$$S_x(t) = \frac{S_0(x+t)}{S_0(x)} = \exp\left\{-\int_x^{x+t} \mu_r \, \mathrm{d}r\right\}$$

$$= \exp\left\{-\int_0^t \mu_{(x+s)} \, \mathrm{d}s\right\}$$

where $\mu(x)$ represents the mortality rate

Survival Function

Survival function must satisfy the following conditions

Condition 1 A life at age x surviving 0 years must have the probability of 1: $S_x(0) = 1$.

Condition 2 All individuals eventually die: $\lim_{t \to \infty} S_x(t) = 0$.

Condition 3 The function of t must be non-increasing: $f'(t) < 0$.

Mortality rate

- Here we are examining whether a concept previously applied to approximation of lightning discharge and ESD currents can also be applied to modelling mortality rates.
- Mortality rate, $\mu(x)$, is the probability of an individual dying at a particular age x.
- Analoguous to *failure rate* for machines.
- Typical observed behaviour: $\mu(x) \sim \frac{1}{x}$ for small x and $\mu(x) \sim e^x$ for large x and has a 'hump' for medium x.
- The rise of the 'hump' is usually interpreted as the transition to adulthood.
- The 'hump' is especially noticeable for men in developed countries.

Logarithm of mortality rate for men in developed countries

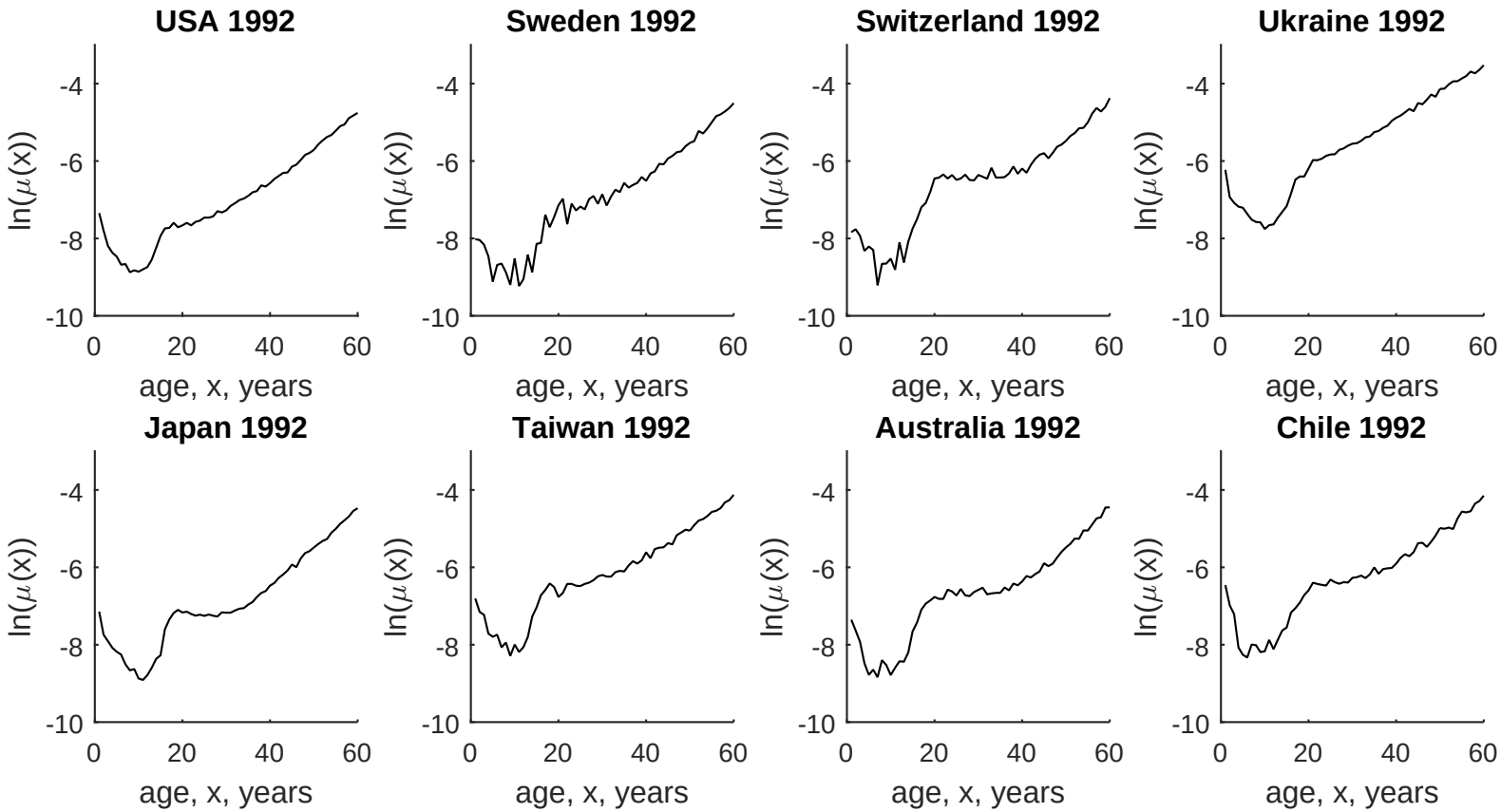

Models of mortality rate

- Many models of mortality rate have been proposed

Model	Mortality rate
Gompertz–Makeham	$\mu(x) = a + be^{cx}$
Double Geometric	$\mu(x) = a + b_1 b_2^x + c_1 c_2^x$
Modified Perks	$\mu(x) = \frac{a}{1 + e^{b-cx}} + d$
Gompertz–inverse Gaussian	$\mu(x) = \frac{e^{a-bx}}{\sqrt{1 + e^{-c+bx}}}$
Weibull	$\mu(x) = \frac{a}{b}\left(\frac{x}{b}\right)^{a-1}$
Logistic	$\mu(x) = \frac{ae^{bx}}{1 + \frac{ac}{b}(e^{bx} - 1)}$
Log-logistic	$\mu(x) = \frac{abx^{a-1}}{1 + bx^a}$

Models of mortality rate

Model	Mortality rate
Thiele	$\mu(x) = a_1 e^{-b_1 x} + a_2 e^{-b_2 \frac{(x-c)^2}{2}} + a_3 e^{b_3 x}$
Heligman–Pollard HP1	$\mu(x) = a_1^{(x+a_2)^{a_3}} + b_1 e^{-b_2 \ln\left(\frac{x}{b_3}\right)^2} + c_1 c_2^x$
Heligman–Pollard HP2	$\mu(x) = a_1^{(x+a_2)^{a_3}} + b_1 e^{-b_2 \ln\left(\frac{x}{b_3}\right)^2} + \frac{c_1 c_2^x}{1 + c_1 c_2^x}$
Heligman–Pollard HP3	$\mu(x) = a_1^{(x+a_2)^{a_3}} + b_1 e^{-b_2 \ln\left(\frac{x}{b_3}\right)^2} + \frac{c_1 c_2^x}{1 + c_3 c_1 c_2^x}$
Heligman–Pollard HP4	$\mu(x) = a_1^{(x+a_2)^{a_3}} + b_1 e^{-b_2 \ln\left(\frac{x}{b_3}\right)^2} + \frac{c_1 c_2^{x^{c_3}}}{1 + c_1 c_2^{x^{c_3}}}$
Hannerz	$\mu(x) = \frac{g(x)e^{G(x)}}{1+e^{G(x)}}$, $g(x) = \frac{a_1}{x^2} + a_2 x + a_3 e^{cx}$, $G(x) = a_0 - \frac{a_1}{x} + \frac{a_2 x^2}{2} + \frac{a_3}{c} e^{cx}$

Model based on power-exponential functions

- We will refer to functions of the form $f(x) = x^a e^{bx}$, $a, b \in \mathbb{R}$ as *power-exponential functions*.
- Using such functions we can build a model with n 'humps'.
- Let $A_n = \{\boldsymbol{a}\} \subset \mathbb{R}^3$ with n elements then the mortality rates is given by

$$\mu(x) = \frac{c_1}{xe^{-c_2 x}} + \sum_{\boldsymbol{a} \in A} a_1 \left(xe^{-a_2 x}\right)^{a_3}.$$

- **Remark:** this model will not model the flattening of the mortality rate for high ages, our main goal is to model the 'hump' well.

Survival function for the proposed model

- Letting T_x denote the time of death the survival function S_x is defined by

$$\Pr[T_x > t] = S_x(t) = \exp\left(-\int_0^t \mu(x+s)\,\mathrm{d}s\right).$$

- Computing S_x for this model gives

$$S_x(t) = \exp\left(c_1\left(\mathrm{Ei}(c_2 x) - \mathrm{Ei}\left(c_2\left(x+t\right)\right)\right)\right.$$
$$\left. \cdot \prod_{a \in A} \exp\left(\frac{a_1}{(a_2 a_3)^{a_3+1}}\left(\gamma(a_3+1, a_2 a_3 x) - \gamma\left(a_3+1, a_2 a_3 (x+t)\right)\right)\right)\right.$$

$\mathrm{Ei}(x) = -\int_{-x}^{\infty} \frac{e^{-s}}{s}\,\mathrm{d}s$ is the exponential integral and $\gamma(a, t) = \int_0^t x^{a-1} e^{-x}\,\mathrm{d}x$ is the lower incomplete Gamma function

Survival function for the proposed model *cont'd*

- Each factor in $S_x(t)$ is non-increasing with respect to t and therefore $S_x(t)$ is non-increasing with respect to t.
- Since $S_x(t)$ is continuous and $S_x(0) = 1$ and $\lim_{t\to\infty} S_x(t) = 0$ both $S_x(t)$ and lifetime cumulative distribution function $F_x(t) = \Pr[T_x \leq t] = 1 - S_x(t)$ have proper boundary behaviour.

Multiple humps

- There are rare examples with multiple humps in the mortality rate

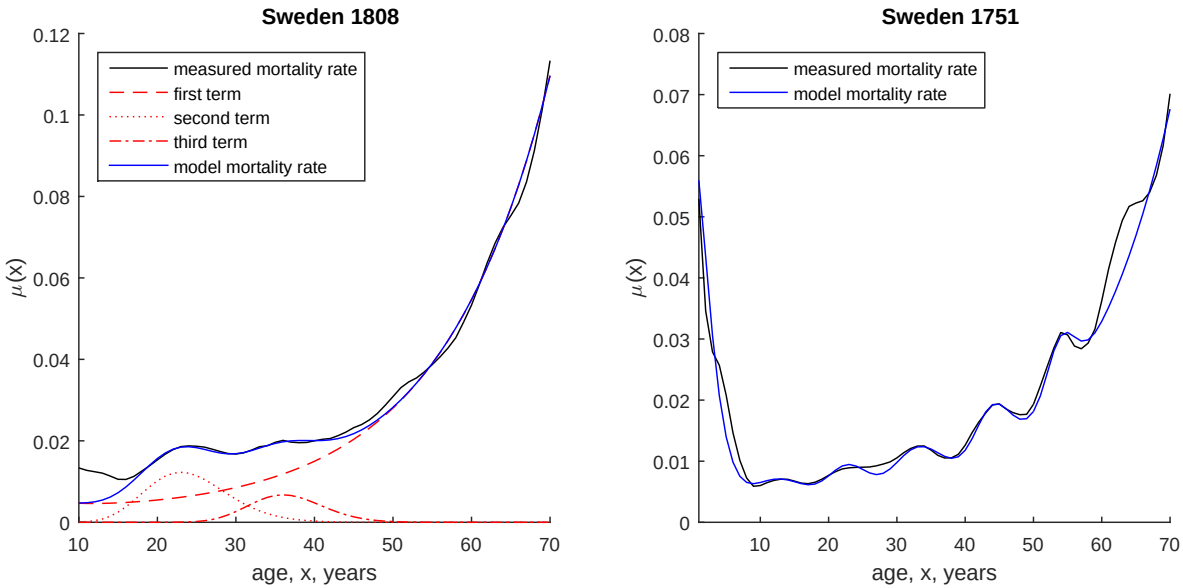

Figure: Examples of a couple of mortality rate curves with multiple humps with model fitted by hand.

- We will only consider the more reasonable and practical single hump case.

Single hump model

- We can model a single hump using
$$\mu(x) = \frac{c_1}{xe^{-c_2 x}} + a_1 \left(xe^{-a_2 x}\right)^{a_3}.$$
- The parameters c_1, c_2 and a_1, a_2, a_3 can easily be interpreted in terms of qualitative properties of the curve.
- To interpret the effects of c_1 note that $\mu(x) \to \frac{c_1}{x}$ when $x \to 0$.
- Looking at $\ln(\mu(x))$ instead we can note that $\frac{\mathrm{d}}{\mathrm{d}x}\ln(\mu(x)) \to c_2$ when $t \to \infty$ so c_2 gives the approximate slope of $\ln(\mu(x))$ for large x.
- $\frac{a_1}{a_2^{a_3}}$ gives the approximate height of the hump, $\frac{1}{a_2}$ gives the time for the humps maximum and a_3 determines the steepness of the hump (the larger a_3 the steeper rise and the faster the decay).

Split single hump model

- c_1 affects the shape of the curve both for high and low ages.
- a_3 affects both the increasing and decreasing part of the hump.
- To avoid this coupling we can split the two terms in the model at their respective local extreme points and adjust the values so that $\mu(x)$ and $\frac{\mathrm{d}\mu}{\mathrm{d}x}$ are continuous,

$$\mu(x) = \frac{c_1}{xe^{-\tilde{c}x}} + a_1 \left(xe^{-a_2 x}\right)^{\tilde{a}} + \Theta\left(x - \frac{1}{c_2}\right) \cdot c_1 \cdot c_2 \cdot \left(e - e^{\frac{c_3}{c_2}}\right) + \Theta\left(x - \frac{1}{a_2}\right) \cdot a_1 \cdot \left(\frac{e^{-a_3}}{a_1^{a_3}} - \frac{e^{-a_4}}{a_1^{a_4}}\right)$$

where

$$\tilde{c} = \begin{cases} c_2, & x \leq \frac{1}{c_2} \\ c_3, & x > \frac{1}{c_2} \end{cases}, \quad \tilde{a} = \begin{cases} a_3, & x \leq \frac{1}{c_2} \\ a_4, & x > \frac{1}{c_2} \end{cases}, \quad \Theta(x) = \begin{cases} 0, & x \leq 0 \\ 1, & x > 0 \end{cases}.$$

Some results

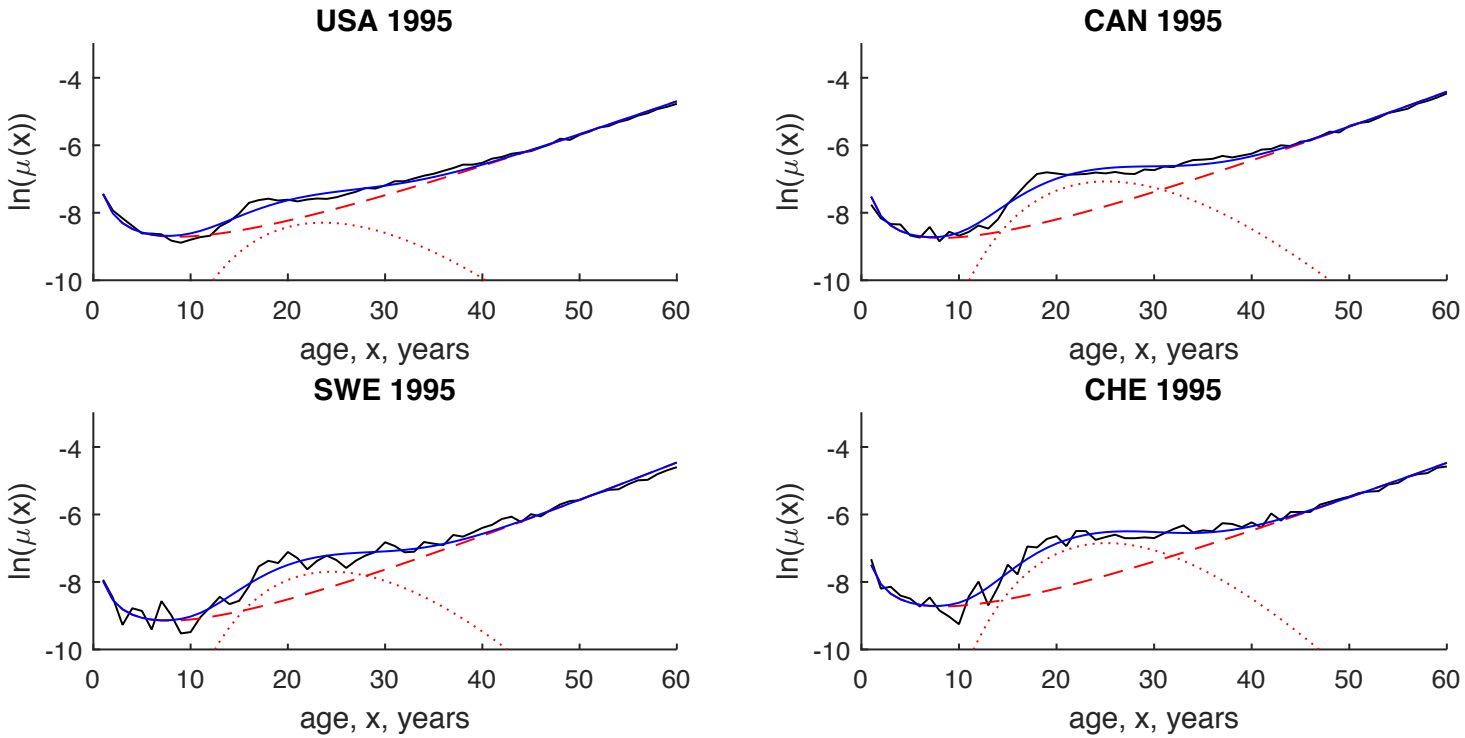

Figure: Examples of a couple of mortality rate curves with multiple humps with fitted model.

Lundengård, Karl, Rančić, Milica and Silvestrov, Sergei. *Modelling mortality rates using power exponential functions.* Mälardalen University, 1-6, SPAS 2017, Oct. 2017.

Some results, cont'd

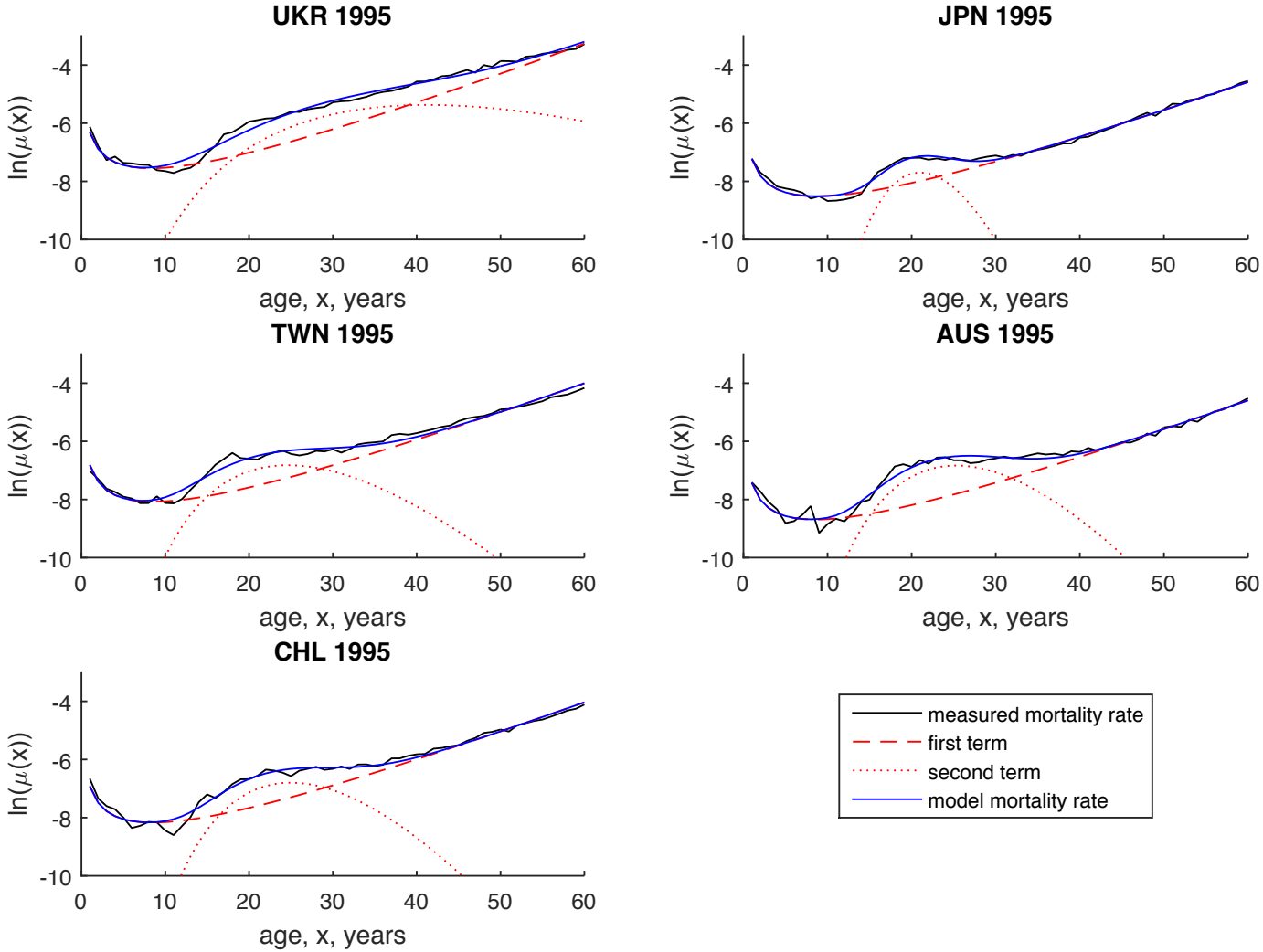

Further work

- Every part of the comparison can be improved
  - More models,
  - More data,
  - Better fitting,
  - Discuss other aspects in more detail such as mortality forecasting (Boulougari, 2018), life insurance pricing (Strass, 2018), pensions or demographics.
- We believe that some sort of systematic comparison of these type of models on a easily available but relevant corpus of data could be a useful and informative tool for researchers and professionals.


Strass, B. (2018). Comparison of prices of life insurances using different mortality rates models (Dissertation). Retrieved from http://urn.kb.se/resolve?urn=urn:nbn:se:mdh:diva-39911


Bouloughari, A. (2018). Application of a power-exponential function based model to mortality rates forecasting (Dissertation). Retrieved from http://urn.kb.se/resolve?urn=urn:nbn:se:mdh:diva-39921

Thank you for your attention!

Questions?

Suggestions?

Contact:
Email: milica.rancic@mdh.se
LinkedIn: https://www.linkedin.com/in/milicarancic/